Open Sea Operating Experience to Reduce Wave Energy Costs

Deliverable D4.3

Floating OWC control algorithms

Lead Beneficiary	TECNALIA
Delivery date	2019-07-30
Dissemination level	Public
Status	Approved
Version	1.0
Keywords	Wave energy, OWC, PTO control, algorithm, MARMOK-A-5

This project has received funding from the European Union's Horizon 2020 research and innovation programme under grant agreement No 654444

Disclaimer

This Deliverable reflects only the author's views and the Agency is not responsible for any use that may be made of the information contained therein

Document Information

Grant Agreement Number	654444
Project Acronym	OPERA
Work Package	WP4
Task(s)	T4.4
Deliverable	D4.3
Title	Floating OWC control algorithms
Author(s)	François-Xavier Faÿ, Joseba Lopez Mendia, Pablo Ruiz-Minguela (Tecnalia), Endika Aldaiturriaga (IDOM), James Kelly (UCC), J. C. C Henriques and L. M. C. Gato (IST)
File Name	OPERA D4.3 - Floating OWC control algorithms.docx

Change Record

Revision	Date	Description	Reviewer
0.1	01-04-2019	Initial outline	Tecnalia
0.2	15-05-2019	First draft	WP4 partners
0.7	20-07-2019	Draft for peer review	University of Edinburgh
1.0	30-07-2019	Reviewed version for submission	EC

EXECUTIVE SUMMARY

The Work Package 4 focused on the design, development, implementation and tests of several control algorithms for Oscillating Water Column technologies in both shoreline and an offshore plant, respectively the Mutriku OWC plant and the Oceantec/IDOM Marmok-A5 buoy installed in BiMEP. The controllers were specifically designed for the novel biradial turbine, an innovative type of self-rectifying radial turbine, and customised for each test infrastructure. The present document, named D4.3 - Floating OWC control algorithms, is the last deliverable of the Work Package. It reports the results of the open sea trials of the control algorithms in BiMEP during Spring 2019.

In brief, the content of the deliverable includes the description of the BiMEP test site, the floating buoy used for the experiment and the Power Take-off system to be controlled. The three tested control algorithms are also detailed, and a performance and reliability assessment is presented based on operational data collected on-site. Additionally, a return on experience is exposed, and recommendations highlighted.

To meet the objectives of the Work Package with the available testing time, the best adaptive and the best predictive algorithms were selected based on the conclusions from the Mutriku testing. Following the naming of the controllers in previous documentation and as listed in the table below, the control algorithms tested were the adaptive controllers CL1 (selected as the baseline), CL2; and the predictive algorithm CL6. Note that CL6 is a first its kind predictive algorithm to be deployed in a WEC using wave measurement up-wave of the device to provide an online optimisation. With the objective of allowing comparison between the controllers, the testing period was divided into two phases where CL1 and CL2 were first operational, followed by CL1 and CL6. During the tests in Spring 2019, the wave buoy positioned up-wave the Marmok measured an average wave of significant wave height of 1.30 m and an average energy period of 7.16 s, which is statistically considered as a calm condition. A total of 900 hours of operation representing a 90% availability of the buoy were secured during the BiMEP test campaign.

SUMMARY OF CONTROL LAWS

Control Law #	Partner	Adaptive/ Predictive	Controls …	Based on …
CL1*	IST	Adaptive	Generator torque	Rotational speed
CL2	UCC	Adaptive	Generator torque	Chamber pressure
CL6	Tecnalia	Predictive	Generator torque	Rotational speed, wave elevation measured up-wave

*CL1 is the baseline controller for CL comparison.

In the performance assessment, the efficiencies of both components composing the drive train, the turbine and generator, as well as the electrical output were derived for each control law.

Additionally, during the Mutriku testing the generator failed and after a repair, an electrical filter was installed between the generator and the power electronics [1]. One consequence of the filter installation was the mandatory change of the type of control in the power electronics to a less accurate one at low operation regions, which induced a drop of the generator efficiency. To overcome this effect, a processing algorithm was developed to select the tests that provided meaningful results for PTO and Control Law performance assessment. As a result of this processing algorithm, 15% of the tests were considered as valid.

Focusing on the turbine performance, a maximum average efficiency of nearly 60% was obtained during the operation of CL6, and the lowest recorded test resulted in a value around 50% for tests operated under CL2. The several versions of CL1 and the CL6 presented similar results in terms of operation ranges and efficiency results. Due to CL2's intrinsic operation behaviour, the tests considered as valid are situated at higher pressure ranges with no common operation point with the baseline controller.

In terms of generator efficiency, CL2 presented valid tests at higher load regime with the highest figures in comparison with the other control laws. Although direct comparison with CL1 would lead to speculation, the trend is CL2 shows better performance in terms of electrical output, although further tests are required to reach a robust conclusion.

Even though CL6 is a predictive algorithm, similarly to CL1, it is based on a torque law approach associating a reference torque to the turbine rotational speed. Based on Mutriku testing results, the algorithm exerted an increase in output power of 30%. However, this was not witnessed in BiMEP and several assumptions are under investigation (accuracy of the wave force estimation and the numerical model, synchronisation between predicted wave train and control actuation) to identify the cause.

Ultimately, the direct comparison between the controllers is weakened by the inability to align the Wave Energy Converter (WEC) production with the wave resource and the selection of valid tests by the processing algorithm.

TABLE OF CONTENTS

LIST OF FIGURES

LIST OF TABLES

ABBREVIATIONS AND ACRONYMS

BiMEP	Biscay Marine Energy Platform
CL	Control Law
GPS	Global Positioning System
IST	Instituto Superior Tecnico
LIFO	Last-In First-Out
MA5	MARMOK-A-5 floating OWC spar-type buoy
MPC	Model Predictive Control
OWC	Oscillating Water Column
PTO	Power Take-Off
SS	Sea States
UCC	University College Cork
WEC	Wave Energy Converter
WP	Work Package

1. INTRODUCTION

The field of wave energy conversion is benefiting from a growing interest around the world with the highest development concentrated in the geographical region of Europe and the United States. To date there have been a limited number of prototypes tested in real conditions and the conclusions of the sea trials are often opaque. The OPERA project aims to share the experience and operational results for four main innovations: two related to the mooring system (shared mooring and elastomeric tethers) and the other two to the energy transformation (Power Take-Off (PTO) system and control algorithms).

Concerning the PTO and control, a first testing phase took place first in the Mutriku Oscillating Water Column (OWC) plant. The novel biradial turbine along with six control algorithms was in operation during a year and results were reported in the previous deliverable D4.2 [1]. Focusing on the control algorithms, two main approaches were considered:

- Generator torque control to adapt the PTO in the best efficiency region;
- Latching control activated by the fast-actuating valve in series with the turbine, whose objective was to affect the damping on the chamber pressure.

Apart from this classification, the control laws (CLs) can be either adaptive or predictive. The adaptive controllers use measured operational data to calculate the control variable and the predictive control uses, in addition to the information of the incoming waves, operational data and a plant numerical model to compute the control parameters.

Following the 1-year testing of the PTO system in the Mutriku OWC plant, the power conversion system was installed inside the MARMOK-A-5 floating OWC spar-type buoy (MA5). Prior to the OPERA project, the buoy was installed in the Biscay Marine Energy Platform (BiMEP) and tested with two Wells turbines. The second buoy deployment accounted for the integration of the 4 main innovations previously cited and offered a way to extend the buoy installation at BiMEP while obtaining operational results.

In comparison with the Mutriku plant, easily accessible for the commissioning and any intervention on-site, the buoy was deployed 4 km off the coast, and any operation was more complex as a result, because they required more aspects to be aligned (availability of weather windows, boat transport, etc). With the new PTO installed in the buoy, system commissioning took longer than expected, as a strong effort was required to ensure system safety. The available testing period was streamlined, and a selection of CLs was developed to facilitate enough tests while complying the task objectives: propose the best in class adaptive and predictive controllers. Following the same numbering as in the deliverable D4.2, the control algorithms tested in the buoy were CL1, CL2 and CL6. To enable control law comparison in the same environmental conditions, there were two testing periods: CL1 vs CL2 and CL1 vs CL6.

In total during the tests, total operational resulted in 900 hours of data for the 3 CLs, during which MA5 was available 90% of the time.

The deliverable is structured as follows:

- Section 2 details the context for testing, mainly the description of the BiMEP test site and the wave resource during the trials, the MA5 buoy and the PTO system;
- Section 3 offers a description of the CLs to be tested and their different versions;
- Section 4 presents the results of the algorithms tested;
- Section 5 reveals some key experiences and the lessons learned during the development and testing of control laws for wave energy conversion;
- Section 6 presents the conclusions of the document and the Work Package (WP) 4.

2. FLOATING WAVE POWER PLANT AT BiMEP

2.1 BIMEP TEST SITE

BiMEP is an infrastructure whose purpose is to test prototypes of marine energy collectors and auxiliary equipment in the open sea. It is located off the coast at Armintza (Spain) with exceptional conditions for testing the effectiveness of new offshore renewable energy concepts and technologies for harnessing wind and wave energy.

The infrastructure is equipped with four 13.2 kV / 5 MW subsea cables fitted with optic fibres and ending in dry mate subsea connectors. It also provided the possibility of connecting devices through a low voltage power (690 V) connection. BiMEP also has an onshore substation fitted with 25 MVA 13.2/132 kV transformers.

The test site area is 5.2 km^2 and is restricted to shipping with perimeter beacons. The depths range from 50 to 90 meters and the seabed is mostly sandy with rocky areas. Figure 1 shows the BiMEP site with the location of the MARMOK-A-5, its mooring perimeter, and the location of the Triaxys wave buoy from which the wave resource is measured.

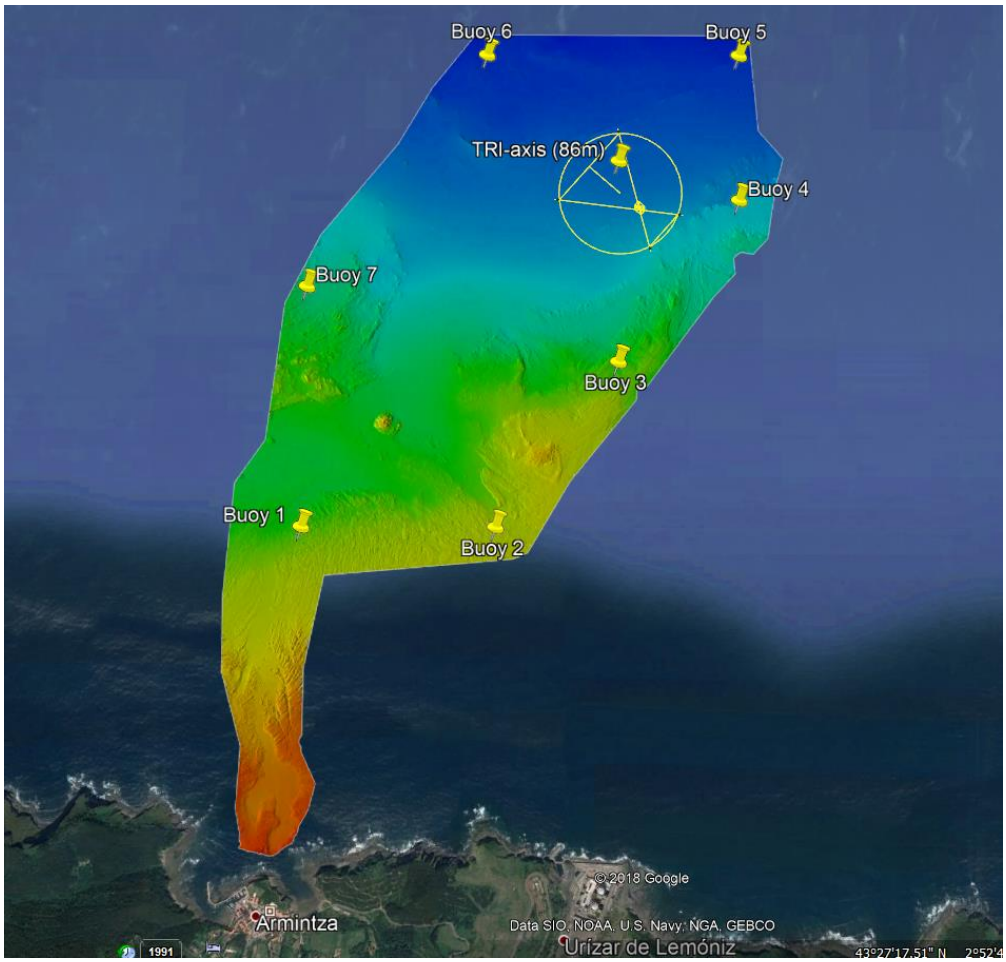

FIGURE 1. BIMEP TEST SITE BATHYMETRY

2.2 WAVE RESOURCE

The wave resource at BiMEP is measured by a series of environmental buoys, one of which was the Triaxys wave buoy illustrated in Figure 2, installed for the OPERA project, and located up-wave from the WEC when considering the most frequent direction of wave propagation. It was used by the predictive controller, CL6, to provide incoming wave data in real-time.

FIGURE 2. TRIAXYS BUOY INSTALLED IN BIMEP

There were two testing periods to allow the comparison of the various controllers: one with CL1 and CL2 operative; the other one with CL1 and CL6. Figure 3 shows the wave resource in terms of significant wave height H_{sig} and energy period T_e covering the two periods. Note that this figure does not represent the actual operation of a CL in a sea state (SS), but the sea states observed during one period or the other. In both cases, the most frequent SS experienced are around $H_{sig} = [0.75 : 1.25]$ m and $T_e = [6.5 : 7]$ s.

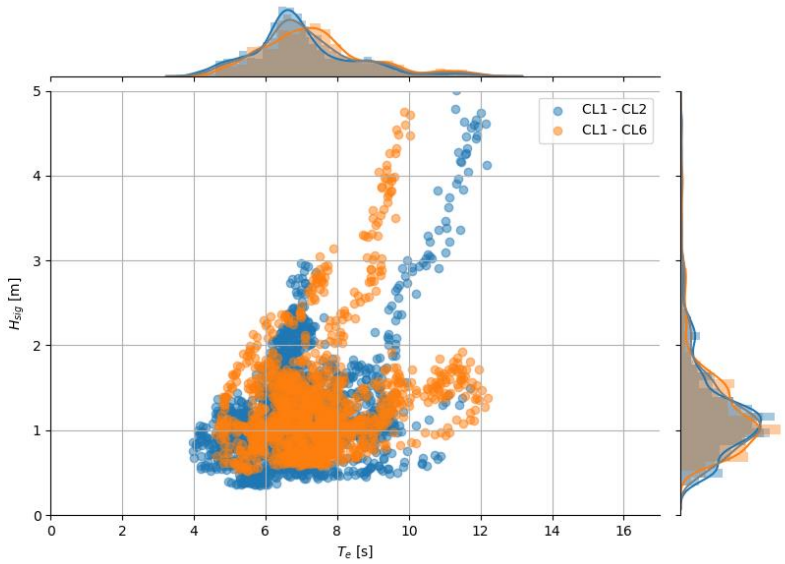

FIGURE 3. SEA STAES COVERING THE TESTING PERIODS

2.3 MARMOK-A-5

MARMOK-A-5 is a spar type OWC WEC buoy. It has a 5 m diameter and is 42 m long; it has a rated power of 30 kW. It was first deployed at BiMEP prior to the OPERA project, with a PTO system consisting of two Wells turbines of 15 kW rated power each.

FIGURE 4. MARMOK-A-5 BASELINE CONFIGURATION

The buoy can be divided into three parts: the floater which adds buoyancy and holds all the electrical equipment and sensors including umbilical cable entry for grid connection; the central cylinder which holds the inner water column; and the water ballast tank which can be partially or fully emptied for buoys transportation and installation/decommissioning.

The mooring system comprises 4 catenary lines with drag anchors which are interconnected by a submerged rectangular cell made of steel wire ropes suspended from 4 pennant surface buoys. The catenary lines are composed of chains and polyester ropes in their top end. MARMOK-A-5 is connected to the submerged cell by 4 polyester ropes. The motivation for using this design is to reduce the number of mooring and anchoring components for arrays of MRE devices, thereby reducing costs and increasing the reliability. Later in the OPERA project, during the second deployment, the two front ropes were substituted by a pair of elastomeric tethers, one of the four main innovations developed during the project.

Another major innovation of the OPERA project is the development and test of a novel biradial turbine. Following an extensive testing campaign in the Mutriku OWC plant documented in [1], [2], it was installed on top of the MARMOK-A-5 buoy, replacing the two Wells turbines. Installation was performed on deck during the buoy refitting. The top cover which held the Wells was replaced by the single biradial turbine.

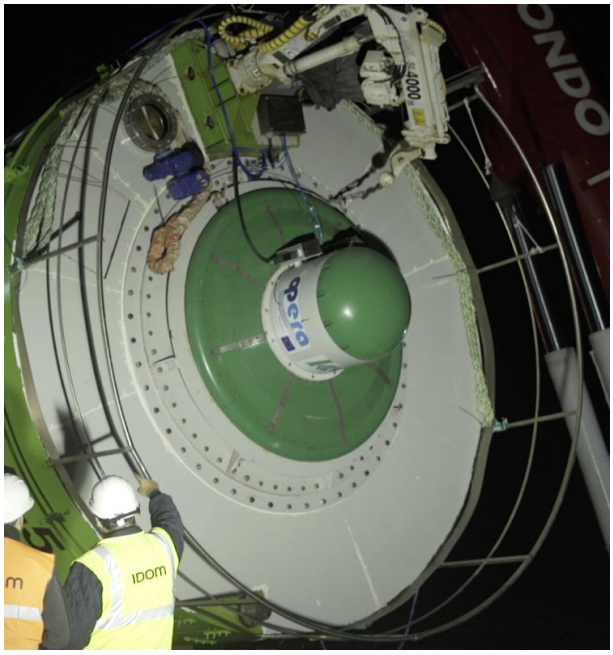

FIGURE 5. BIRADIAL TURBINE INSTALLED ONSHORE BEFORE TOW IN

FIGURE 6. BIRADIAL TURBINE IN OPERATION AT BIMEP

2.4 POWER TAKE-OFF SYSTEM

2.4.1 AIR TURBINE

The turbine- performance can be described by the dimensionless aerodynamic parameters of pressure head Ψ, mass flow rate Φ, power Π and efficiency η expressed as in [3] as a function of the air chamber pressure p_{ch} , the mass flow rate $\dot{m}_{\mathrm{t}}$ and P_{t} the turbine shaft power.

$$\Psi = \frac{p_{ch}}{\rho_{\mathrm{in}}\Omega^2 d^2}, \qquad (1)$$

$$\Phi = \frac{\dot{m}_t}{\rho_{in}\,\Omega\,d^3} = f_\Phi(\Psi), \tag{2}$$

$$\Pi = \frac{P_t}{\rho_{in}\Omega^3 d^5} = f_\Pi(\Psi), \tag{3}$$

$$\eta = \frac{P_t}{p_{ch}Q_t} = \frac{\Pi}{\Psi\Phi}. \tag{4}$$

Here d is the turbine diameter and Ω is the rotational speed in $\mathrm{rad/s}$, and ρ_{in} is the inlet density at stagnation conditions. In the present report, the following approximation was used

$$\rho_{in} = \rho_{at}, \tag{5}$$

where ρ_{at} is the air density at a pressure of 101325 Pa and a temperature of 288 K. This approximation is expected to reduce the turbine power in about 2 to 3% with respect to conditions usually found in laboratory. The torque provided by the turbine is simply $T_t = P_t/\Omega$.

The diameter and inertia of the biradial turbine that was initially installed in Mutriku wave power plant (see Figure 7) and then later on the MARMOK-A-5 device are shown in Table 1.

TABLE 1. TURBINE CHARACTERISTICS

Parameters	Symbol	Value	Unit
Diameter	*d*	0.50	m
Total inertia of turbo-generator set	***I***	5.01	kg m^2

FIGURE 7. TURBINE INSTALLED IN MUTRIKU WAVE POWER PLANT

The turbine characteristics $\Phi = f(\Psi)$, also known as turbine damping, and $\eta = f(\Psi)$ are plotted in Figure 8.

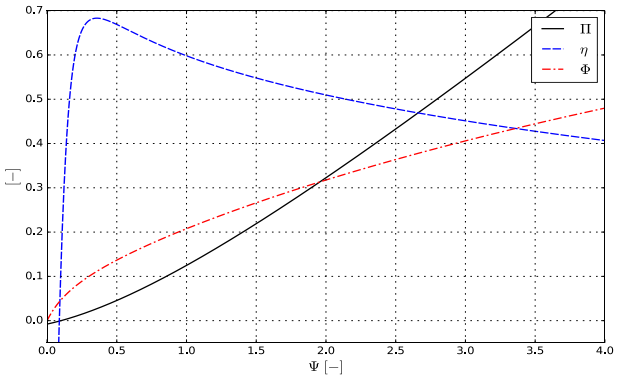

FIGURE 8. PERFORMANCE CURVES OF OPERA BIRADIAL TURBINE. DIMENSIONLESS FLOW RATE Φ, POWER COEFFICIENT Π AND EFFICIENCY η VERSUS DIMENSIONLESS PRESSURE HEAD Ψ. BASED ON DATA FROM [4].

2.4.2 ELECTRICAL GENERATOR

The electrical generator installed as part of the PTO is an asynchronous induction generator with a rated power of 30 kW, whose characteristics are extracted from [1] and listed in Table 2.

TABLE 2. GENERATOR SPECIFICATIONS

Parameters	Symbol	Value	Unit
Rated power	P_{nom}	30	kW
Rated torque	T_{nom}	195	Nm
Rated speed	N_{nom}	1470	rpm
Maximum speed	N_{run}	3000	rpm
Insulation class	Class	H (180 °C)	-
Number of pole pairs	N_{pp}	2	-
Mass	m_{gen}	250	kg
Nominal voltage	V_{nom}	400	V
Frequency	f_{hz}	50	Hz

2.4.3 SAFETY VALVE FOR CONTROL OF THE TURBINE

A safety valve installed in the turbine operates in high energetic sea states to protect the components. It prevents the turbine from reaching over-speed. If the threshold of the cut-off speed Ω_{co} is reached, the valve closes and blocks the air flow. A torque is applied at the generator following the present control law and reduces the rotational speed until a cut-in speed Ω_{ci} is reached. When this value is reached, the valve opens, and the turbine resumes normal operation. The valve actuation time was initially around 0.1 s when the latching algorithms were tested in Mutriku and was raised to 1 s for safety reasons. Table 3 below presents the values to control the safety valve:

TABLE 3. OPERATION OF THE SAFETY VALVE

Parameters	Symbol	Value	Unit
Valve closure rotational speed	Ω_{co}	220	rad/s
Valve re-open rotational speed	Ω_{ci}	180	rad/s

2.4.4 POWER ELECTRONICS AND CONTROL SYSTEM

Power electronics Unidrive M series were implemented as the back-to-back converter. The system is formed by a 132 kW AC/DC regenerative dispositive and a DC/AC drive of 90 kW. The regenerative drive is connected to the grid through an LCL filter and uses 690 Vac as feed voltage. Power is then transported to the onshore substation by means of the umbilical cable. Reactive power control is performed in the regenerative drive to ensure minimum voltage disturbances and a stable DC link voltage.

The drive unit used the sine filter (LC) already used in Mutriku for protecting the generator. This was not used during MARMOK-A-5's first deployment and had to be incorporated during the maintenance works in the shipyard.

The Programmable Logic Controller (PLC) installed was in charge of several critical tasks for the correct operation of the complete WEC system:

- Process data acquisition from field components (pressure, internal water level, temperature sensors, etc);
- Communicate with the Variable Frequency Drive in a fast a reliable way to correctly control the power extraction from the generator. This was done by means of Ethernet/IP protocol using a 10 Hz heartbeat rate;
- Control the safety aspects of the power capture and trigger safety procedures if necessary (i.e. safely turn down the power electronics and close HSSV valve);
- Control the safety valve system to perform safety and control-level operations (i.e. latching/unlatching;
- Postprocess data to be presented to the SCADA system.

The selected PLC, a 600MHz CPU unit from Austrian manufacturer Bernecker&Rainer offered a very good performance without any major issue. Moreover, it showed excellent operability and was a centrepiece across the 3 control laws testes in the buoy.

Communication with the HSSV controller was implemented by means of Modbus/TCP standard.

Oceantec/IDOM had previously worked in the control software framework that implements the overarching state machine to control PTO operation, plant safety and acquisition system. This enabled the seamless integration of the control laws as tested in Mutriku to the code deployed in the wave energy converter.

3. CONTROL ALGORITHMS DESCRIPTION

The three control laws are detailed in this section. CL1 and CL2 were adaptive controllers using respectively the turbine rotational speed and the internal chamber pressure as drivers to compute the generator torque demand. CL6 was a predictive law, similar to CL1, but using the real-time data of incoming waves and optimising the control parameters online.

TABLE 4. SUMMARY OF THE CONTROL LAWS

Control Law #	Partner	Adaptive/ Predictive	Controls …	Based on …
CL1*	IST	Adaptive	Generator torque	Rotational speed
CL2	UCC	Adaptive	Generator torque	Chamber pressure
CL6	Tecnalia	Predictive	Generator torque	Rotational speed and wave elevation from Triaxys

*CL1 is the baseline controller for CL comparison.

3.1 CL1: ADAPTIVE GENERATOR TORQUE CONTROL BASED ON ROTATIONAL SPEED

3.1.1 DESCRIPTION

Following the definition of power coefficient (see Section AIR TURBINE 2.4.1), CL1 control law was based on simple evidence that the turbine power extraction, $\mathrm{P_t}$, should be proportional to

$$\mathrm{P_t} \propto \Omega^3, \tag{6}$$

if the turbine inertia is very low. If the inertia is non-negligible, the following control law is proposed to define the generator power:

$$P_{\mathrm{gen}} = a\,\Omega^{\mathrm{b}}, \tag{7}$$

where a and b are two constants that depend on the turbine geometry and the inertia of the turbine and the generator rotating parts.

Two variations of the control law were implemented. The first applied directly with an upper limit to the instantaneous generator power,

$$P_{\mathrm{gen}}(\Omega) = \min\left(a\,\Omega^{\mathrm{b}}, P_{\mathrm{gen}}^{\mathrm{rated}}\right). \tag{8}$$

Here a and b are user defined constants and $P_{\mathrm{gen}}^{\mathrm{rated}}$ is the generator rated power, see Figure 9. If the turbine rotational speed reaches Ω_{max} then the system enters in safe mode and the valve is closed until the rotational speed drops below Ω_{thr}, resuming the system to normal operation.

A second version aimed to reach less often the generator rated power, $P_{\text{gen}}^{\text{rated}}$. As such, a stepping increase of the generator power was applied above the rotational speed threshold Ω_{thr1}

$$P_{\text{gen}}(\Omega) = \begin{cases} a_1 \Omega^{b_1}, & 0 < \Omega < \Omega_{\text{thr1}}, \\ a_2 \Omega^{b_2}, & \Omega_{\text{thr1}} < \Omega < \Omega_{\text{thr2}}, \\ P_{\text{gen}}^{\text{rated}}, & \Omega_{\text{thr2}} < \Omega, \end{cases} \tag{9}$$

where a_1 and b_1, Ω_{thr1} and Ω_{thr2} are user defined constants. The constants a_2 and b_2 are computed such that the control law function is continuous between Ω_{thr1} and Ω_{thr2}, see Figure 10. As in the case of the previous version of the CL1, if the turbine rotational speed reaches Ω_{max} then the system enters in safe mode and the valve is closed until the rotational drops below Ω_{thr1}, resuming the system to normal operation.

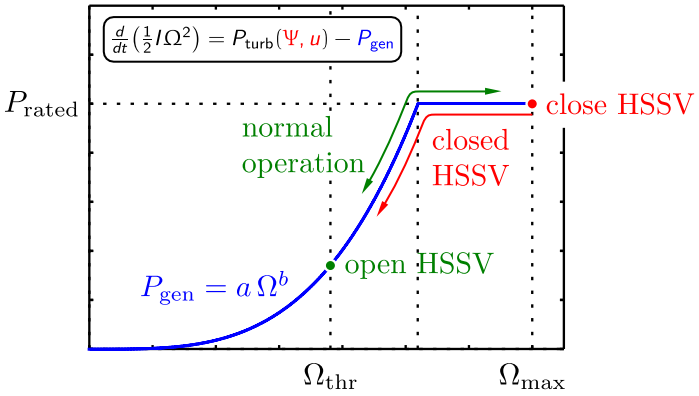

FIGURE 9. BASE VERSION OF THE CONTROL LAW CL1

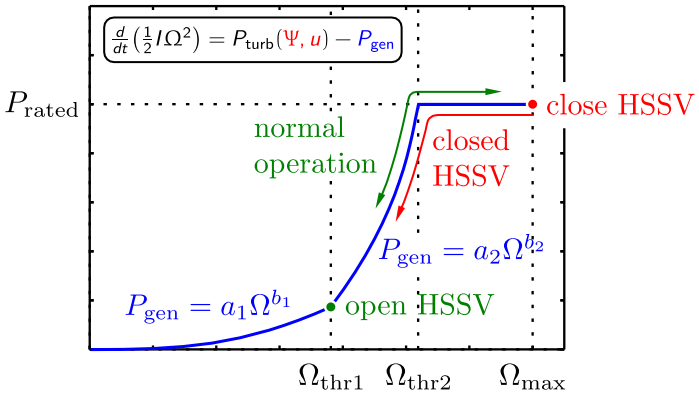

FIGURE 10. STEPPER VERSION OF THE CONTROL LAW CL1

3.1.2 REQUIREMENTS

The CL1 minimum input requirement is the measurement of the biradial turbine rotational speed, Ω, at a sampling frequency of 4 Hz. The output is the generator torque computed as

$$T_{\text{ctrl}} = P_{\text{gen}}\,\Omega^{-1}, \tag{10}$$

The other requirement of CL1 is the instantaneous valve position if operating in safe mode.

3.2 CL2: ADAPTIVE GENERATOR TORQUE CONTROL BASED ON CHAMBER PRESSURE

3.2.1 DESCRIPTION

Control Law CL2 resulted in a quasi-constant torque reference that changed slowly as the mean chamber pressure changed. The primary goal of the control law was to maintain good average aerodynamic efficiency of the turbine, while minimising stress to the generator and power electronics of the PTO. With a slow changing reference torque, rapid fluctuations in power capture were momentarily stored in turbine inertia. Equation *(11)* is the initial control law, which is referred to as CL2.1, as described.

$$T_{\text{ctrl}} = \text{k}_0 + \text{k}_1\overline{p_{\text{ch}}} + \text{k}_2\overline{p_{\text{ch}}}^2 + \text{k}_3\overline{p_{\text{ch}}}^3 \qquad (11)$$

where T_{ctrl} is the reference torque and $\overline{p_{\text{ch}}}$ is the mean chamber pressure. The moving average was taken over a period of 5 minutes and continually updated throughout the operational period. The value of k_1 was selected to maximise efficiency of the turbine at a given pressure, and it was calculated based on the turbine curves. The values of k_0, k_2, and k_3, were set to zero. The coefficient k_1 was determined based on calculations performed on the turbine operating at a flow coefficient of 0.14, where the turbine operated at a calculated efficiency of 63%, which was just beyond the maximum efficiency of 64% at a flow coefficient of 0.12.

Initial operation of CL2 revealed that during higher energy sea state conditions, the turbine inertia could not absorb enough of the excess energy, which causes the turbine to overspeed. A revised mean pressure-based control law introduced a fifth coefficient based on instantaneous chamber pressure. This term was added to increase the reference torque during pressure peaks to minimise turbine overspeed in higher energy sea conditions while maintaining the torque reference from *(11)* as a floor. The updated controller, which is referred to as CL2.2, is represented in *(12)*.

$$T_{\text{ctrl}} = \text{k}_0 + \text{k}_1\overline{p_{\text{ch}}} + \text{k}_2\overline{p_{\text{ch}}}^2 + \text{k}_3\overline{p_{ch}}^3 + \text{k}_4(|p_{\text{ch}}| - \overline{p_{\text{ch}}}) \qquad (12)$$

where p_{ch} is the instantaneous chamber pressure.

The control law for this project also included a rotational speed 'floor', where if the rotational speed of turbine was below a set value, no torque would be applied to the generator. The floor can be adjusted depending on sea state conditions as well as generator specifications to maximise energy conversion efficiency during operation. The value of k_4 was selected to minimise overspeed of the turbine during operation, and the value of the rotational speed floor was selected based on generator specifications and sea state conditions.

Further testing indicated the added k_4 term was insufficient at controlling overspeed while maintaining maximum system efficiency over a range of sea states. CL2 was adjusted further with the terms for k_2, k_3 and k_4 being replaced by merging the k_3 and k_4 to create *(13)*, which was the final version of CL2 testing in the MARMOK-A-5.

$$T_{\mathrm{ctrl}} = \mathrm{k}_0 + \mathrm{k}_1\overline{p_{\mathrm{ch}}} + \left(\mathrm{k}_5\overline{p_{\mathrm{ch}}}^3\right)(|P_{\mathrm{ch}}| - \overline{p_{\mathrm{ch}}}) \qquad (13)$$

3.2.2 REQUIREMENTS

3.2.2.1 DESIRABLE REQUIREMENTS

- Voltage on the DC Link of the back to back power converter (If measured, this can be used to determine, offline, any flexibility offered by using the dc-link to smooth speed fluctuations.);
- Accurate real-time measurement of the pressure drop across the turbine;
- Confirmation that guide vanes are fully open (will help in sanity checks);
- Temperature of power electronics and of generator;
- Burst of very high-resolution measurements of voltages, currents. E.g. 200 ms window of data recorded at a sample rate high enough to determine harmonics on 50 Hz, e.g. 1 kHz sampling or greater.

3.2.2.2 MINIMUM REQUIREMENTS

- Mean measurement of chamber pressure;
- Instantaneous chamber pressure;
- Instantaneous rotational speed;
- Real-time turbine mechanical rotational speed;
- Ability to run the generator drive in torque control mode.

3.3 CL6: NON-LINEAR MODEL PREDICTIVE CONTROL FOR GENERATOR TORQUE CONTROL

3.3.1 DESCRIPTION

3.3.1.1 THE OPTIMISATION ALGORITHM

CL6 was a non-linear model predictive control (MPC) algorithm operated using real-time data from the measurement buoy to optimise online the control vector $u' = [a, b]$ of the torque law:

$$T_{\mathrm{ctrl}} = \mathrm{a}\,\Omega^{\mathrm{b}} \qquad (14)$$

MPC algorithms have a high computational cost as they require an optimisation at each sample over the prediction horizon. The proposed control strategy was inspired by this philosophy but was computationally lighter because the optimisation was made at each re-planning time T_{rp}, determined as half the prediction horizon, and relied on a heuristic algorithm for the optimisation. This prediction horizon T_{ph} was the time available to perform the online optimisation. Figure 11 details the time framework of the algorithm. At time t the optimisation was run over the prediction horizon until t'. The control vector u' was then used by the control law during the full re-planning time t_1, and so on.

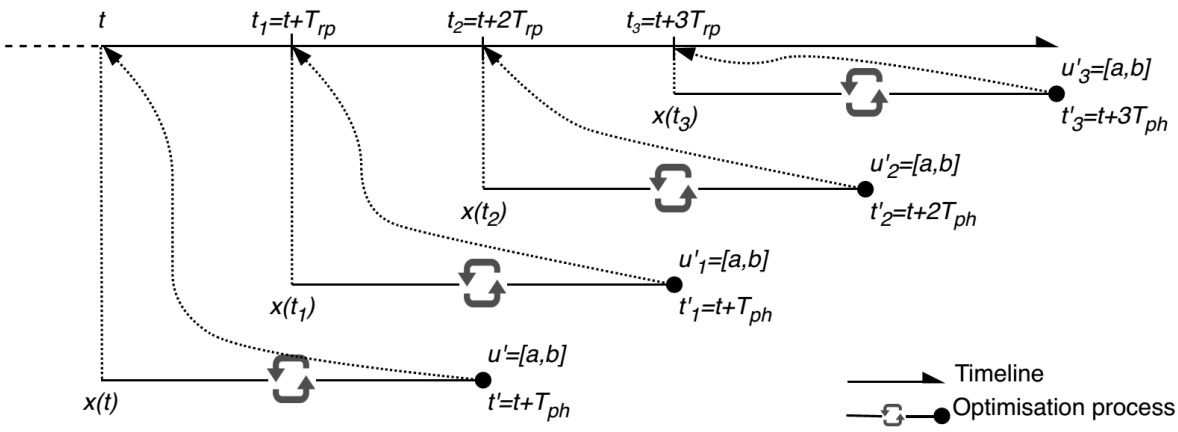

FIGURE 11. RECEDING TIME FRAMEWORK OF THE PREDICTIVE ALGORITHM

At each re-planning period, the online optimisation process was run. It comprised a heuristic search with vectors of possible candidates of $\boldsymbol{a}$ and $\boldsymbol{b}$ which evolves **+/-Δ$\boldsymbol{a}$** and **+/-Δ$\mathbf{b}$** centered around the previous optimised parameters. This avoids sudden changes of torque law and guided the search of the new control coefficients.

The objective function to be minimised included the various power conversion steps from the pneumatic P_{pneu}, to mechanical P_{turb}, to the electrical power P_{gen}.

$$J = \min\left(-\frac{1}{T_{\mathrm{ph}}}\int_{t}^{t+T_{\mathrm{ph}}}(\alpha\, P_{\mathrm{pneu}} + \beta\, P_{\mathrm{turb}} + \gamma\, P_{\mathrm{gen}})\right) \qquad (15)$$

α, β and γ are weighting parameters to set different levels of priority in the conversion chain.

3.3.1.2 PREDICTION AND ESTIMATION OF THE WAVE FORCES

In practice, the maximum time for the prediction depended on the wave propagation time from the measurement buoy to the WEC. To avoid over complicating the process, the propagation time varied in function of the distance between the two buoys and the wave period. Before each test, the wave buoy and the WEC sent their GPS coordinates and the propagation distance $\boldsymbol{d_{T2M}}$ was calculated. The wave velocity $\boldsymbol{c}$ was calculated knowing the

wave period and the water depth following Figure 12 from the DNV recommendation RP-C205 [5]:

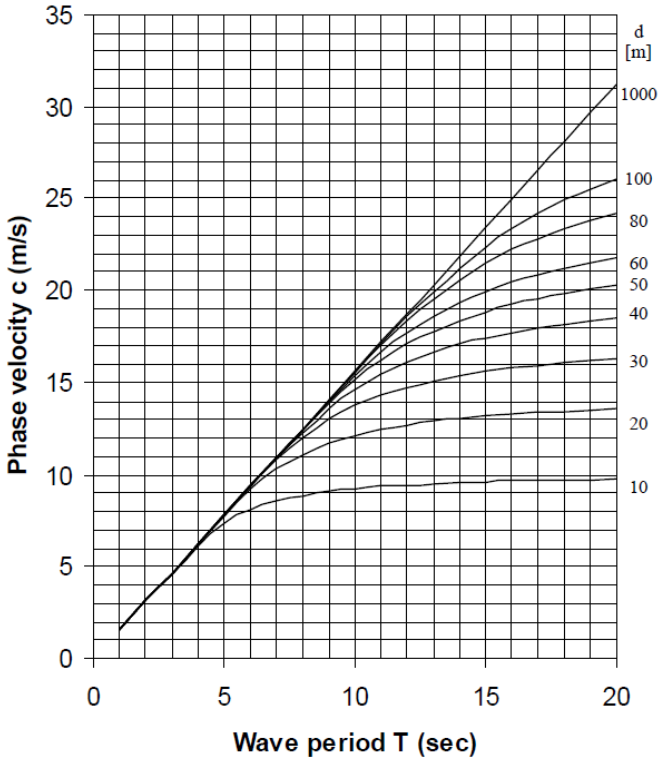

FIGURE 12. WAVE VELOCITY IN FUNCTION OF THE PERIOD AND DEPTH – FROM [5]

For the water depth $d = 80\ m$ where the WEC was installed, the wave phase velocity was defined by the polynomial:

$$c = \mathrm{a_c}\, T^2 + \mathrm{b_c}\, T + \mathrm{c_c} \qquad (16)$$

With the coefficients $\mathrm{a_c} = -0.03972, \mathrm{b_c} = 0.0863$ and $\mathrm{c_c} = -1.2983$.

Finally, the wave travel time, and thus the prediction horizon, was given by:

$$T_{\mathrm{ph}} = d_{\mathrm{T2M}}/c \qquad (17)$$

Before triggering the optimisation, the algorithm required a vector of the excitation forces of the incoming waves representing the wave forces exerted on both the buoy structure and the internal water column. The wave elevation was measured by the wave buoy and sent to the control in real-time at 2 Hz. It was re-sampled at 10Hz, the frequency of the model, while filling a moving vector of the size of the prediction horizon. The estimation of the excitation forces

$\hat{F}_{\mathrm{exc,i}}$ was done for each mechanical body i (1: buoy structure, 2: internal water surface) following the theory presented in [6], [7]:

$$\hat{F}_{\mathrm{exc,i}}(t) = k_{\mathrm{t,i}}(t) * \eta_{\mathrm{w}}(t) = k_{\mathrm{t,i}}(t - t_c) * \eta_{\mathrm{w}}(t + t_c) = k_{\mathrm{t,i,c}}(t) * \eta_{\mathrm{w,p}}(t) \qquad (18)$$

Where $k_{\mathrm{t,c}}(t)$ is the causal complex excitation impulse response function (EIRF) and $\eta_{\mathrm{w,p}}(t)$ the predicted wave with the t_{c} causal time. That way both amplitudes and phases were considered. The convolution was resolved in the time domain by approximating the EIRF with the Prony method at 5$^{\mathrm{th}}$ order for each body and calculated by a state-space system. Figure 13 shows in simulation a comparison of a wave excitation force and its respective wave elevation computed from a wave spectrum versus the estimated one computed from the same wave elevation for a sea state $H_{\mathrm{s}} = 2.78\ \mathrm{m}$ and $T_{\mathrm{p}} = 15.88\ \mathrm{s}$. The estimation for the structure is similar although not precisely accurate, but this estimation was deemed satisfactory to include in the predictive model.

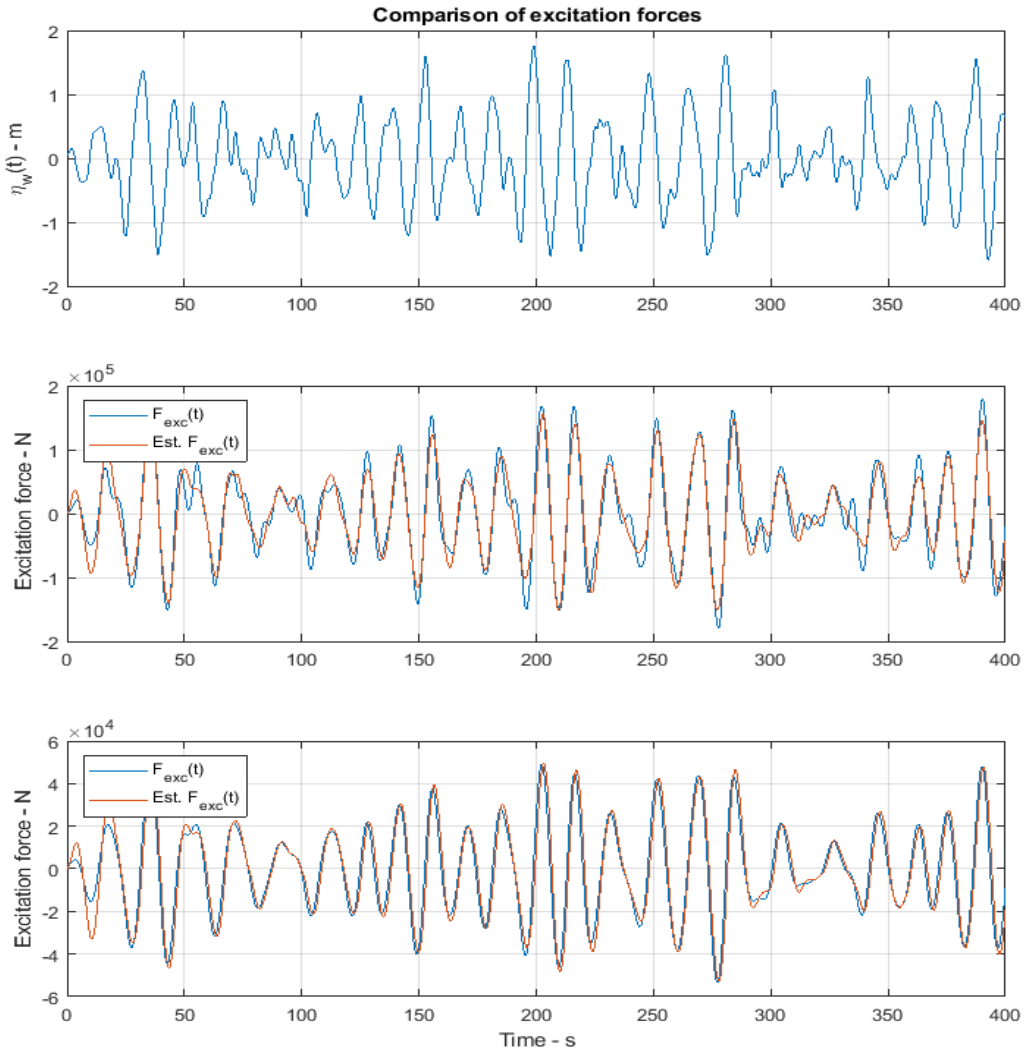

FIGURE 13. COMPARISON OF EXCITATION FORCES AND THEIR ESTIMATIONS FOR THE STRUCTURE (MIDDLE) AND THE WATER COLUMN (BOTTOM) USING THE WAVE ELEVATION (TOP)

Figure 14 shows in practice the wave measured at the wave buoy and the equivalent wave forces estimated for a full 30-minutes test and zoomed in (500 s – 600 s) for a sea state $H_s = 1\ m, T_e = 6\ s$.

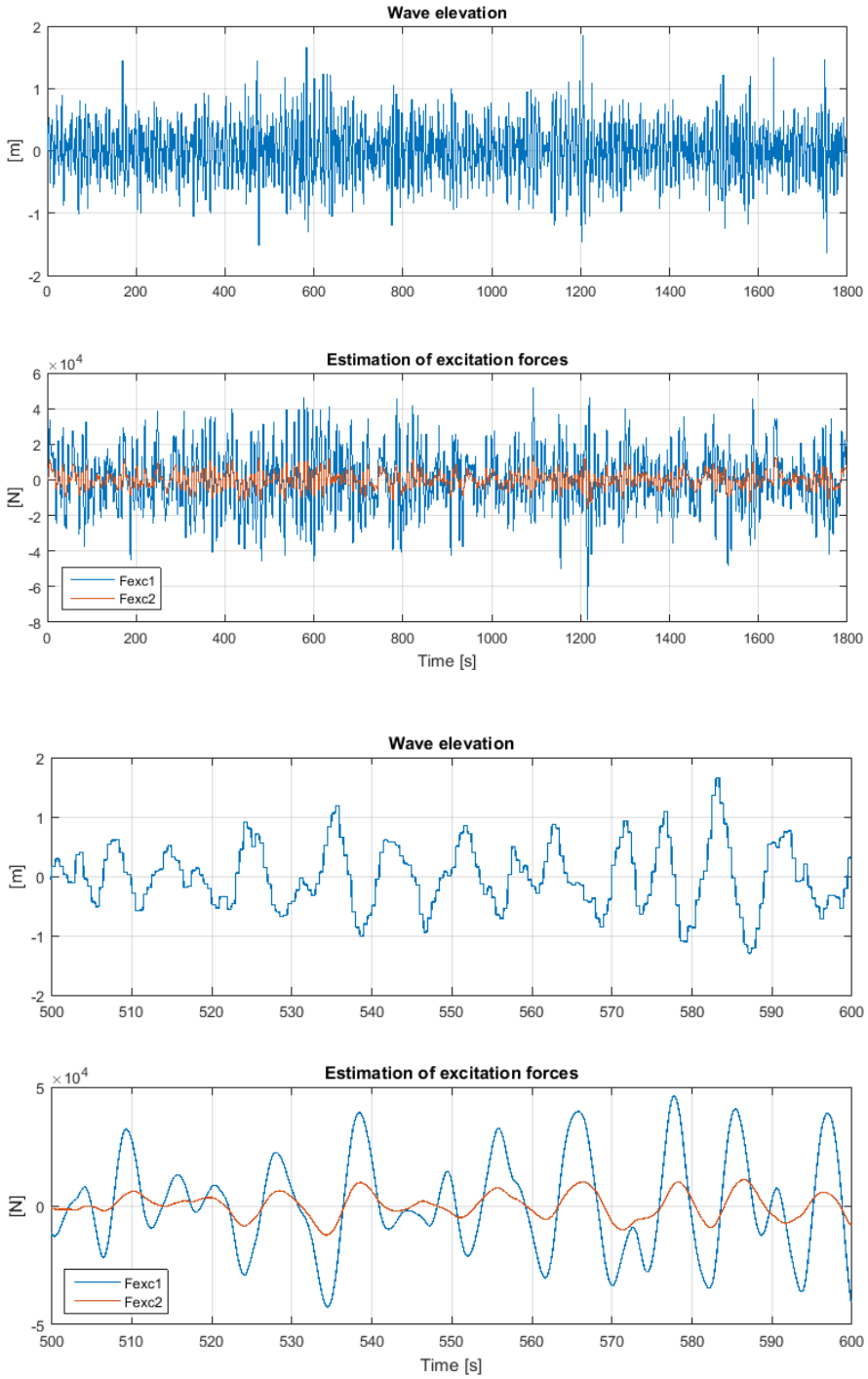

FIGURE 14. WAVE ELEVATION FROM THE WAVE BUOY AND EXCITATION FORCE ESTIMATION

PREDICTIVE CONTROL REQUIREMENTS

Before the MPC was run, a series of variables had to be initialised with a mix of measured and calculated quantities. The model state vector was composed of 6 states and amplified with the radiation coefficients:

$$x = [v_1\ v_2\ x_1\ x_2\ p\ \Omega \mid Rad] \quad (19)$$

The first 6 states were given by local measurements from the PLC where v_1 and v_2 were respectively the buoy structure and the internal water surface heave velocity, x_1 and x_2 their positions, p is the internal chamber pressure and Ω the turbine rotational speed. The vector Rad represents the different radiation states used to compute the radiation forces. Similarly, to the excitation forces, these can't be measured, and a virtual sensor estimating these had to be modelled, so the radiation forces are computed by the model.

At each time instant, a wave elevation was measured by the Triaxys buoy, and the wave excitation forces were updated in the sliding vector of forces following a LIFO method (Last-In First-Out). The wave propagated until reaching the buoy and the associated forces were then the first elements of the vector of excitation forces. Knowing the excitation forces, the buoy motion, the pressure and the turbine speed, the radiation forces were computed and so were the states Rad in the state vector which initialises the MPC.

3.3.2 REQUIREMENTS

This algorithm used both measurement from the MA5 and data from the wave buoy. The minimum requirements of CL6 are presented in Table 5:

TABLE 5. MINIMUM REQUIREMENT OF CL6

Measurement	Specification
MA5 buoy structure and water column motion in the chamber (position and speed)	Real-time
Pressure in chamber	
Turbine speed	
Wave elevation from the wave buoy	with minimum 1 wave period prediction

In addition to these basic needs, the algorithm needed an accurate hydrodynamic model and an exact PTO characterisation. The more accurate the model, the better the optimisation which is:

- The prediction of the excitation force: using the wave measurement buoy located in front of the MARMOK-A-5, the wave forces were estimated for the duration of the wave travel time;
- A validated numerical model: used during the optimisation process.

4. IMPLEMENTATION, TEST RESULTS AND ANALYSIS

During the first phase of the OPERA project, the PTO and six control algorithms were tested in the Mutriku OWC plant. Moving to BiMEP for the second phase of the project, the objective for the offshore testing was to test the best adaptive and the best predictive controller with a particular focus on potential safety issues.

Three controllers were selected, upon which CL1 is taken as the base case to compare both CL2 and CL6. This selection was supported by a reduced testing period and the necessity to rely on a sufficient amount of operational data to analyse the results. The control algorithm testing calendar was tied to the completion of the commissioning of all the equipment and sub-systems integrated in the WEC. Delays were experienced at the PTO commissioning, that, although the PTO had been extensively tested for a full year at the Mutriku plant, could not be foreseen. The offshore tests took place in Spring 2019, a period during which the MARMOK-A-5 successfully operated autonomously with an availability rate of 90% during when the control laws were automatically switched. Almost 900h of operational data were collected during the two testing periods:

- Phase 1 with CL1 and CL2;
- Phase 2 with CL1 and CL6.

TABLE 6. OPERATION DATE AND DURATION OF CLs

CL#	Started operation	Hours
1	03/05/2019	406
2	03/05/2019	280
6	29/05/2019	207
Total hours of operation		893

In total, 2239 tests were performed during the CL testing period and operated simultaneously to allow comparison. Before showing the results of the performance of all CLs with respect to their ability to control the PTO, Figure 15 shows the captured power as a function of the internal pressure variations for the entire set of tests. The pneumatic power represents the energy captured by the buoy and is weakly affected by the control. There is a trend common to all CL proving the tests were operational during the same environmental conditions.

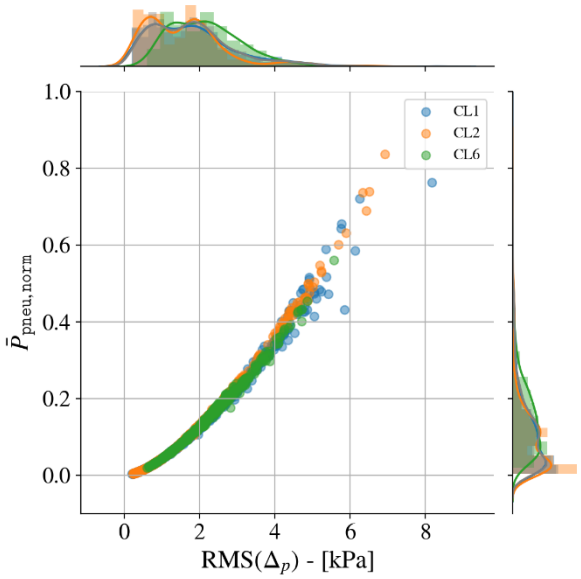

FIGURE 15. PNEUMATIC POWER IN FUNCTION OF THE CHAMBER PRESSURE FOR THE ENTIRE SET OF TESTS

4.1 INTRODUCTION TO DATA ANALYSIS

During the Mutriku testing, at the end of September 2017, an overvoltage damaged the electrical generator. After the generator was repaired with a reinforced stator insulation, the manufacturer advised the installation of a filter between the generator and the power electronics to prevent the failure from occurring again. This advice was followed and the device maintained operation in Mutriku Phase II and in BiMEP. However, the only drawback with the installation of the filter was the necessity to change the inner current control of the power electronics from closed-loop to open-loop which is less efficient and accurate. This control applies the reference torque, calculated by the CL and sent by the PLC to the power electronics, which sets as reference the equivalent current to extract from the generator.

In Deliverable D4.2 [1], a drop of the PTO efficiency was observed between Phase I, no filter, to Phase II, after the generator was reinstalled. But at that time the cause is not fully understood. A deeper analysis revealed that at low torque and low speed, the reference torque fails to be accurately applied. This does not prevent control laws from running, but actually blurs the real extracted torque and power measurements.

A processing algorithm was developed to select the events during which the control was applied correctly. The operational data from Mutriku Phase II and BiMEP were post-processed using this approach. The reader is kindly asked to read the Deliverable D3.4 where the complete processing algorithm is detailed. Especially Figures 11 and 12 from D3.4 exhibit the effect on both the turbine and the generator performance. From the 2239 tests, 358 were selected by the post processing methodology.

The installation of the d*V*/d*t* filter and the change of the electronics control mode between the two phases of testing at Mutriku, had a minor effect on the turbine performance and significant impact on the electrical generator efficiency, see Figure 16 and Figure 17.

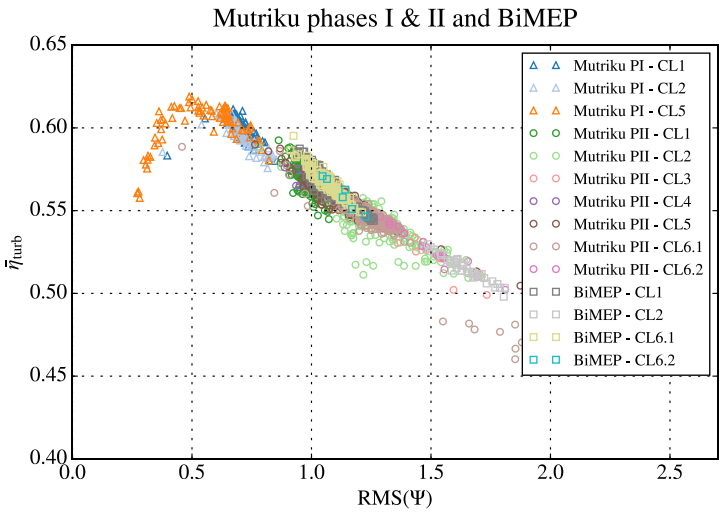

FIGURE 16. - TAKEN FROM D3.4 - BIRADIAL TURBINE TIME-AVERAGED EFFICIENCY RESULTS FOR MUTRIKU PHASES I & II AND BIMEP. IN THE LEGEND, PI AND PII DENOTES PHASE I AND PHASE II.

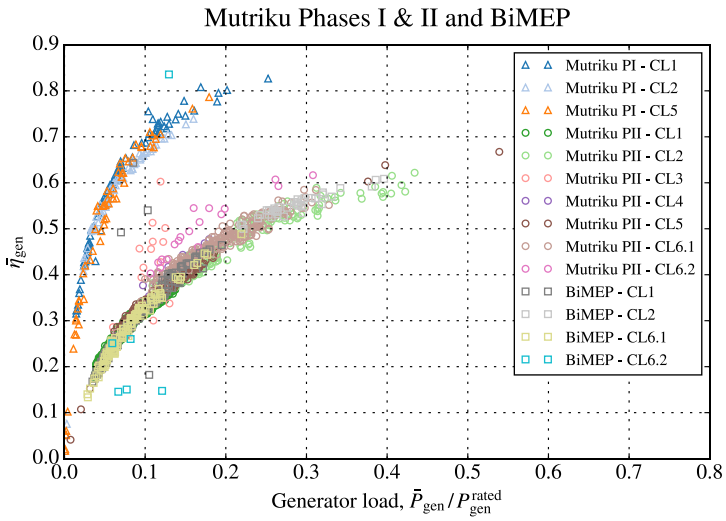

FIGURE 17. - TAKEN FROM D3.4 - ELECTRICAL GENERATOR TIME-AVERAGED EFFICIENCY RESULTS FOR MUTRIKU PHASES I & II AND BIMEP. IN THE LEGEND, PI AND PII DENOTES PHASE I AND PHASE II.

4.2 ASSESSMENT OF THE CL COVERING THE DEPLOYMENT AT BIMEP

In Deliverable D5.3 [8], a wave by wave analysis concluded that there is not much difference in average output power when selecting time scales from few hours to 5 minutes. For the data analysis, 10-minute blocks were considered initially, and was later raised to 30 minutes. The total number of individual tests resulted in 2239 and are detailed by CL in Table 7.

TABLE 7. NUMBER OF TESTS PER CL

CL	N. of elements
1	1042
2	783
6	414

4.2.1 PHASE 1: CL1 – CL2

4.2.1.1 IMPLEMENTATION OF CL1 AND CL2 IN THE PLC

For CL1 and CL2, the control algorithms are not very complex and simple lines of codes directly coded into the PLC are enough to compute the reference control torque. Several versions of CL1, labelled CL1.x, were tested, and CL2 was tuned to maximise power output performance and eventually a second version of the algorithm was developed and tested to allow the control law to make more complete adjustments to the changing sea conditions. In the data presented, the first algorithm is identified as CL2.1 and the second algorithm is identified as CL2.2, see Section 3.2. Due to the sea conditions and processing thresholds, only one trial dataset from CL2.2 was available to be evaluated for PTO performance.

4.2.1.2 COMPARISON OF THE PTO PERFORMANCE

The control laws CL1 and CL2 deployed on the MARMOK-A-5 follow the same pattern of performance found at the Mutriku Wave Power Plant, see [1]. The application of CL2 resulted in higher average generator torques, which resulted in lower average rotational speeds and higher average values RMS-Ψ when compared to CL1. The lower rotational speeds increased the values of RMS-Ψ leading to lower average efficiencies for the pneumatic-to-mechanical power conversion of the turbine, see Figure 18-A. Additionally, the grouping of the measured RMS-Δ_p is less uniform as shown in Figure 18-B. CL2 torque calculation is not influenced by turbine speed, but rather turbine pressure, which results in a wider variety of RMS-Δ_p. The recorded values are seen in Figure 18-B are much more scattered than those reported for CL1, which indicates that CL2 results in less consistent turbine efficiencies than CL1 over the same values for RMS-Δ_p.

Due to the inaccuracies in the application of the reference torque by the open-loop control and of measuring current by the power electronics that control the generator, only a small number of datasets produced could be considered to have accurately and faithfully applied each control law. The criteria for identifying tests where the CLs were accurately applied limited the CL2 tests to those which occurred at higher energy seas, which resulted in higher values of RMS-Δ_p and higher mechanical power produced.

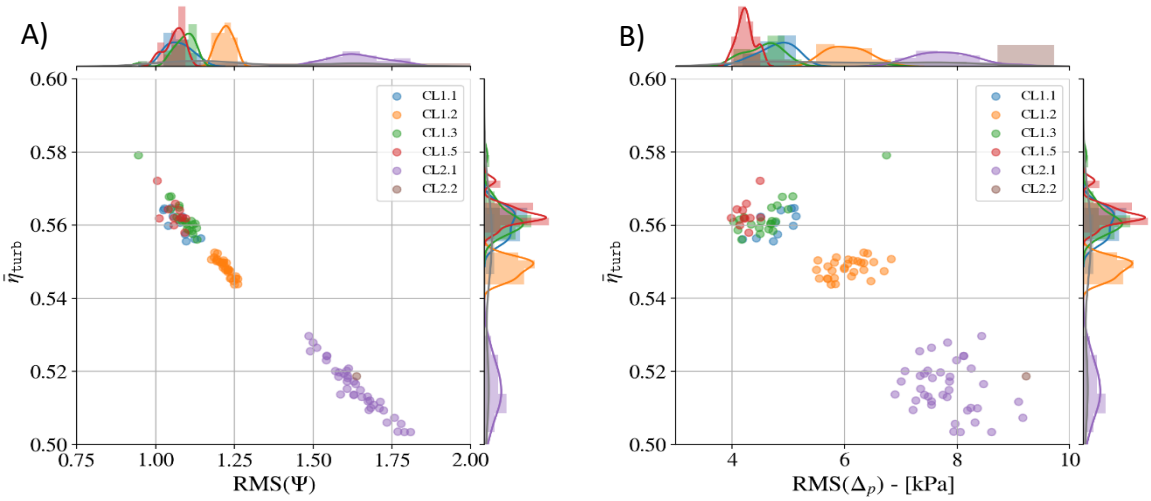

FIGURE 18. CL1-CL2 COMPARISON OF AVERAGE TURBINE EFFICIENCY IN FUNCTION OF A) THE DIMENSIONLESS PRESSURE AND B) THE PRESSURE VARIATIONS

Figure 19 indicates that the lowest average normalised turbine power for CL2 was approximately 0.43, a value that was never observed in a valid CL1 test. The highest average turbine power was associated with CL2.2, in the only test of CL2.2 that met the performance thresholds for evaluation. The problems associated with data accuracy and the different sea state conditions meant it was difficult to directly compare the performance of the selected CL1 and CL2 tests.

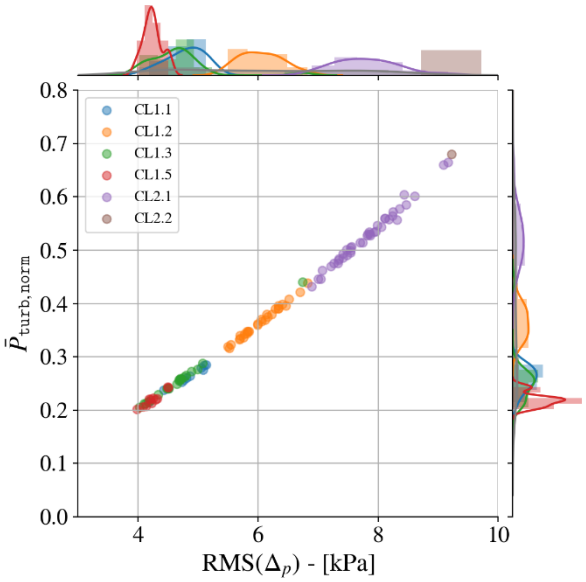

FIGURE 19. CL1-CL2 COMPARISON OF AVERAGE TURBINE POWER

Like the results of the Mutriku Phase II tests, the largest advantage that CL2 offered relates to the generator performance. Compared to CL1, the CL2 algorithm produces higher reference torques and higher average generator loads, which allowed the generator to operate at higher efficiencies as indicated in Figure 20. As the application of CL2 resulted in evaluated datasets

with significantly higher RMS-Δ_p and higher turbine powers, the CL2 algorithm also resulted in higher electrical power generation. The increased electrical generation is presented in Figure 21, which indicates that the lowest average electrical output from CL2 testing is higher than the highest average electrical output from CL1 testing. These results reinforce the findings from the Mutriku Phase II tests that CL2, while resulting in lower turbine efficiencies, produced higher generator efficiencies. The increase in generator efficiencies of CL2 appear to outweigh the losses in turbine efficiencies, and this suggests for instants where the controller relies on open-loop, approximation-based controllers that CL2 is a better option than CL1. The open-loop generator control, which was a result of the *dV/dt* filter, and the lack of overlapping conditions between the CL1 and CL2 tests that can confidently be evaluated, makes it challenging to reach definitive conclusions on performance comparisons between the two control laws. The effect of the electrical filter introduces another level of uncertainty in the experimental results.

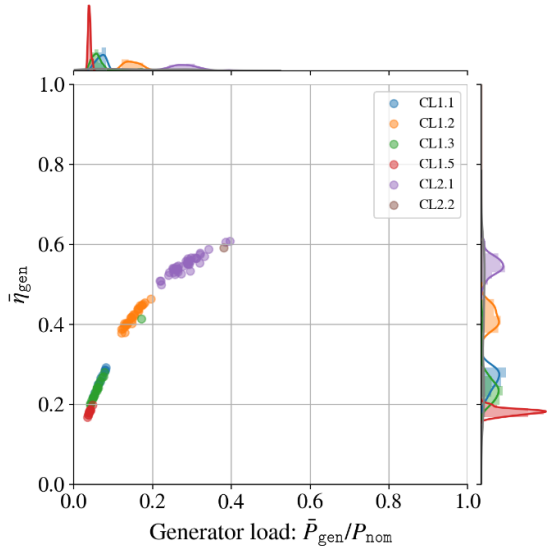

FIGURE 20. CL1-CL2 COMPARISON OF AVERAGE GENERATOR EFFICIENCY VERSUS THE ELECTRICAL LOAD

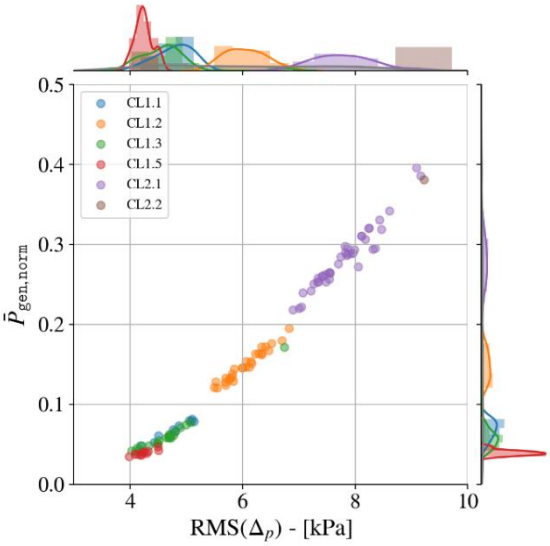

FIGURE 21. CL1-CL2 COMPARISON OF AVERAGE GENERATOR POWER VERSUS THE PRESSURE VARIATIONS

4.2.2 PHASE 2: CL1 – CL6

The 2nd phase in the BiMEP testing lasted for two weeks. This section compares only the CL1 tests recorded during this period with CL6 tests. No CL2 tests were performed during this 2nd phase.

4.2.2.1 IMPLEMENTATION OF CL6 IN THE CONTROL FRAMEWORK

From one side, the wave data (sea state statistics and real time wave elevation) are sent to shore by the Triaxys buoy via a VHF radio link (Very High Frequency). The antenna receiving these data is installed on-shore in the surveillance mast of BiMEP and linked to the onshore PC, located in the BiMEP offices, with fibre optics and then with a serial connection. Figure 22 displays the software used to send commands to the buoy and receive the real time wave elevation data (acceleration, position and zero-crossing period).

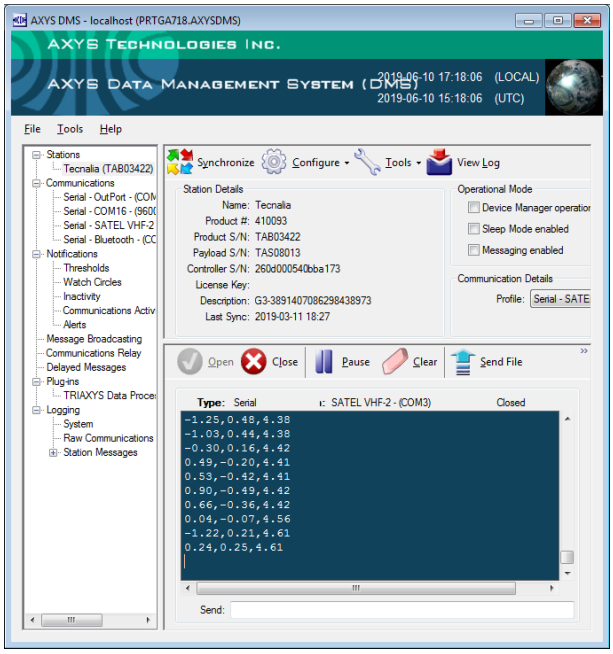

FIGURE 22. SOFTWARE TO COMMUNICATE WITH THE WAVE BUOY

From the other side, the PLC was located on-board in the MA5 buoy and connected to shore via the fibre optics wires of the electrical export cable.

There are two versions of the CL6 algorithm:

- **CL6.1**: the optimisation process is done by the onshore PC to avoid too many constraints on the PLC computation burden;
- **CL6.2**: the algorithm is lightened so the optimisation can run on the PLC directly.

For CL6.1, the onshore PC received data from both sides, executed the algorithm and sent back the control parameters to the PLC which applied the new control law. For CL6.2, the onshore PC received the data from the wave buoy and sent them to the PLC which computed the optimisation algorithm and applied the control law.

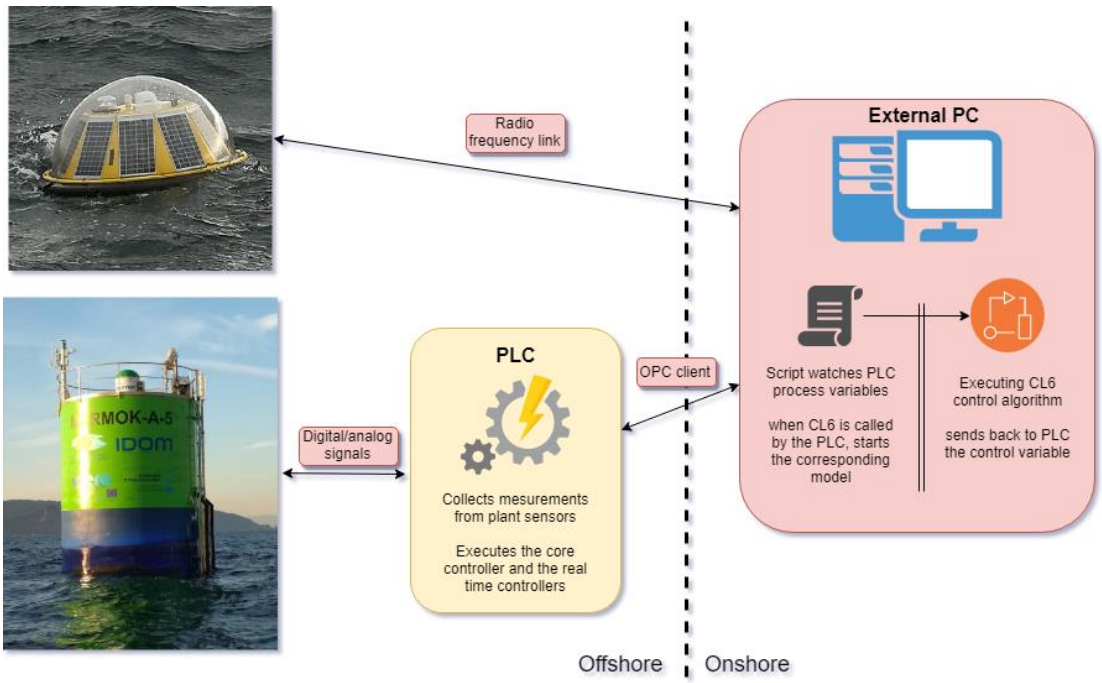

FIGURE 23. CONTROL FRAMEWORK AT BIMEP SITE

When the wave buoy was sending real-time the wave resource signals to shore, the stress on the batteries was more demanding. To indicate the charge of the battery pack and the effect of CL6 operation. Figure 24 presents the battery voltage in normal operation and during real time transmission for the predictive law. The batteries were powered by solar panels and the voltage variation was due to the solar irradiance, charging, and its operation mode, discharging.

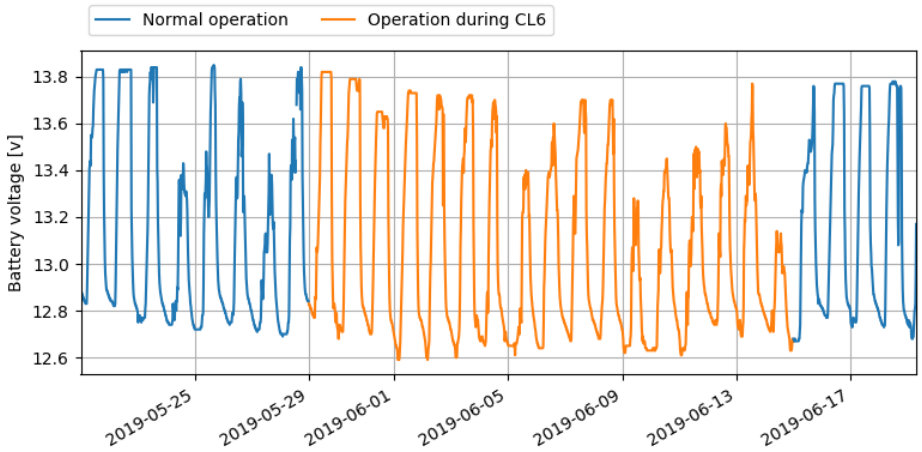

FIGURE 24. BATTERY CHARGE WITH AND WITHOUT THE REAL TIME DATA TRANSMISSION

When operating with the real time transmission on, the voltage decreases day after day and the sun cannot fully charge them during day hours. However, it never falls below the threshold value of 80% of the full capacity, where the buoy enters in sleep mode.

The validation of both the implementation and the control algorithm was achieved by two convergence tests presented in Figure 25. For both tests, the control parameters were willingly set far from the optimal value and the evolution is observed during 3h and 6h. The sea states are reported in Table 8.

TABLE 8. SEA STATES DURING THE CONVERGENCE TESTS

Test #	$H_s\ [m]$	$T_e[s]$
1	0.75 to 1.00	7.5 to 8.5
2	0.65 to 0.80	6.5 to 7.5

The two tests were done during sea states quite similar. In both cases the control parameters evolve in a short time period representing the local optimised parameters, and in a longer period are converging to the same values, oscillating close to $a \approx 2.10^{-4}$ and $b \approx 2.25$.

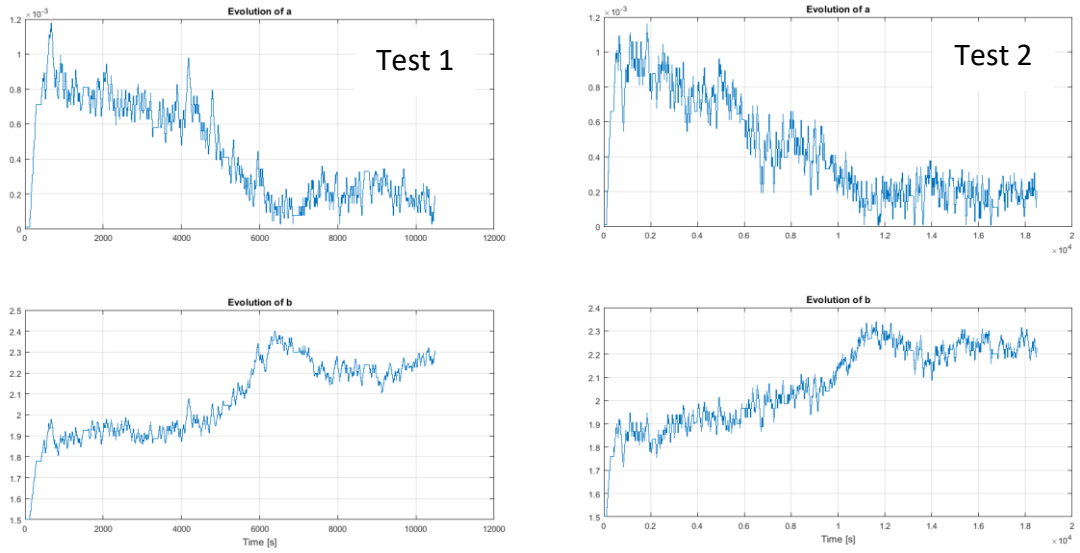

FIGURE 25. CONVERGENCE TESTS FOR THE VALIDATION OF CL6 IMPLEMENTATION

In practice, a change of the [*a,b*] control parameters represents a new torque law curve. Within a same test, and depending on the environmental conditions, the combination of [*a,b*] may not vary – c.f. Figure 26. Two cases-A) the instantaneous torque values follow a unique trend, low energetic conditions – and on the opposite can present high variations – c.f. Figure 26-B) the instantaneous torque values populate the entire figure. This could be witnessed for example in high energetic conditions when a set of big waves was followed by a set of calm waves, thus proving the ability of the control to adapt to these fast-changing conditions. This shows the versatility of the control and the constant adaptation to wave conditions.

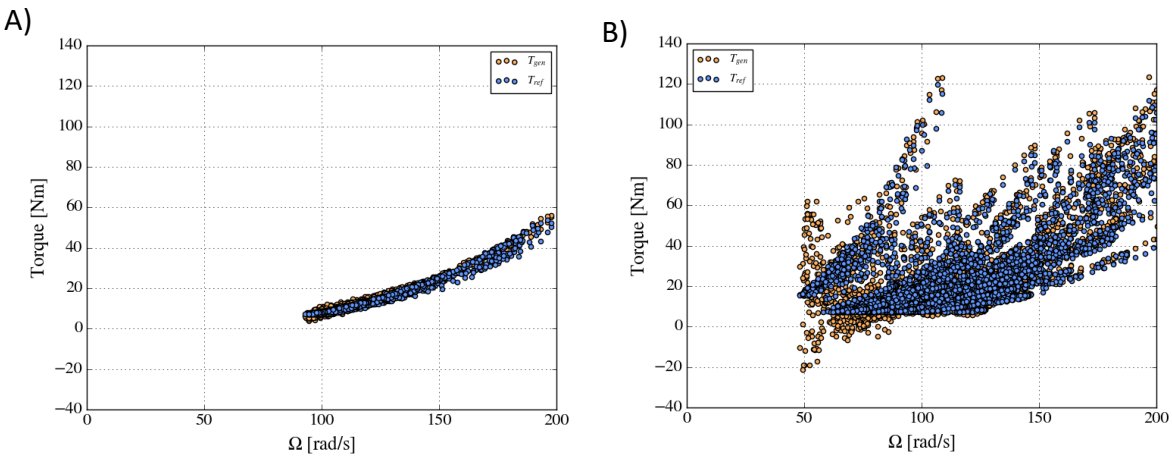

FIGURE 26. TWO CASES WITH DIFFERENT BEHAVIOUR OF THE PREDICTIVE ALGORITHM CL6

4.2.2.2 COMPARISON OF THE PTO PERFORMANCE

This section presents and compare the biradial turbine performance under the different versions of CL1 and CL6. While the CL1 versions constitute a change in the control parameters, CL6 versions are two different implementation techniques in the control system.

Focusing on CL6.1, the average turbine efficiency falls in the range 55 to 60% including the highest efficiency recorded for an individual test (c.f. Figure 27 A) and B)). There are only few CL6.2 points which makes it difficult to assess. CL1 and CL6 have quite similar behaviour, they both rely on torque laws even if they use different control parameters. The results show homogeneous performance and a comparison is directly possible. Figure 27-C) offers a way to compare CL6 with a bin assessment, each bin is 0.1 kPa and with CL1 as the reference. Globally, the relative difference is in the range +4/-3% and a trend showing slightly better performance of CL1 at higher pressure variations.

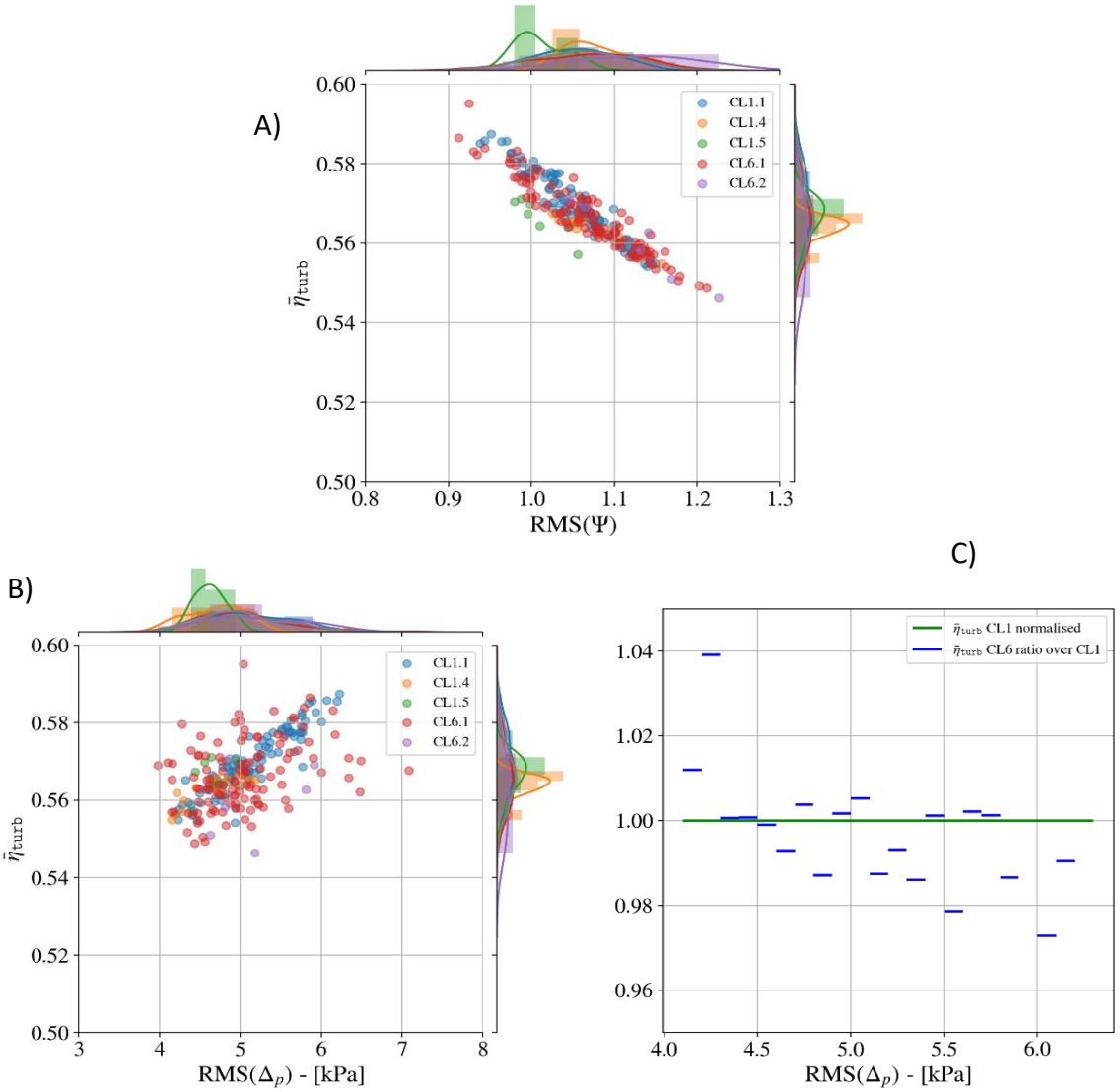

FIGURE 27. CL1-CL6 AVERAGE TURBINE EFFICIENCY VERSUS: A) DIMENSIONLESS PRESSURE B) PRESSURE VARIATION AND C) THE BIN COMPARISON OF CL6 AGAINST CL1

In terms of mean turbine power production presented in Figure 28, there is clearly a linear trend with both CL and their versions. The only notable fact in terms of performance comparison is that some CL6 tests operate at higher pressure values and thus the mean production is higher in these cases.

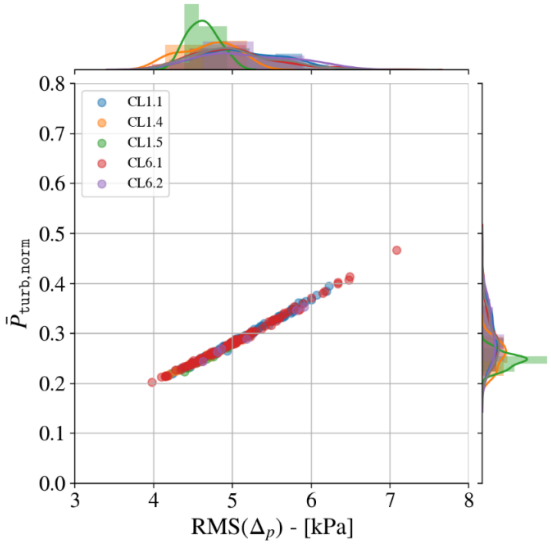

FIGURE 28. CL1-CL6 AVERAGE TURBINE POWER PRODUCTION VERSUS PRESSURE VARIATION

The generator performance can be seen in Figure 29. As the mean electrical load is increasing, so is the average generator efficiency. At best it reaches 50% for CL6.1 close to a 20% load whereas CL1 does not present results with load higher than 15% so the efficiency is a not reaching more than 40%, values following the global trend for both CL. Note that CL1 and CL6.2 present few outliers outside the common trend. In the bin comparison showing results of CL6 against CL1, the range of relative difference is +7/-7% almost equally distributed in positive and negative values. The comparison is not possible for average loads higher than 15% where only CL6 is present. At higher loads CL6 shows slightly higher generator efficiencies while at the same time the turbine efficiency decreases a bit. It should be noted that the generator efficiency curve during the operation at Mutriku Phase I was significantly higher than in Mutriku Phase II and BiMEP. As a result, the conclusions drawn for Mutriku Phase II and BiMEP are valid when the d*V*/d*t* is installed.

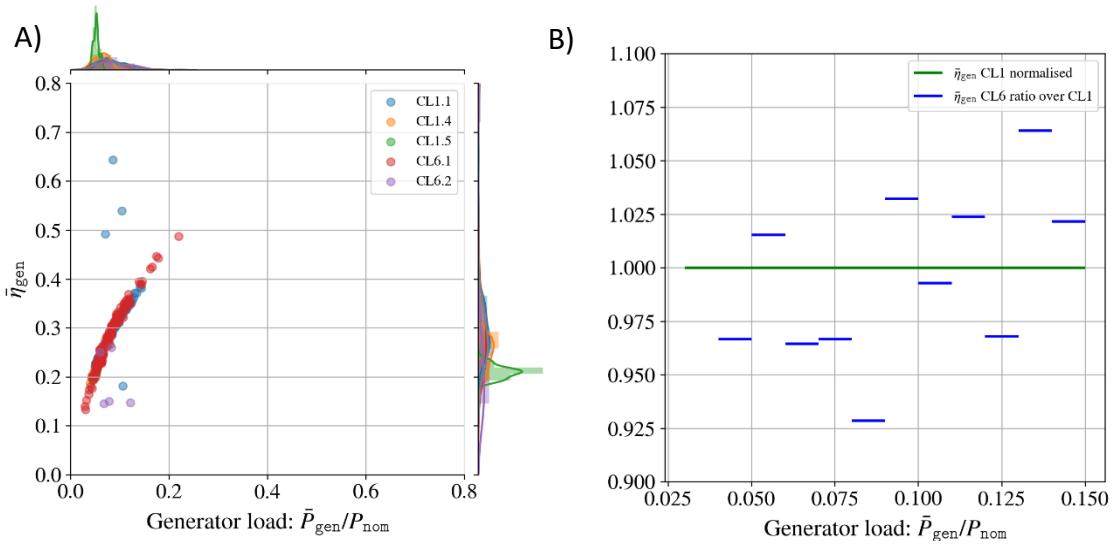

FIGURE 29. CL1-CL6 COMPARISON OF AVERAGE GENERATOR EFFICIENCY: A) IN FUNCTION OF THE ELECTRICAL LOAD AND B) WITH BIN COMPARISON

The generator average power production is plotted, in Figure 30, as a function of the RMS pressure variations. It should be noted that the pneumatic power is mainly a monotonic function of the available pressure head. The values of power are quite low because the tests were performed during two weeks of mainly low energetic sea states. The trend seems to show an improvement in the electrical power production from CL6 over CL1 especially when operating at RMS pressure ranges over 5 kPa, reaching at best 10%. Note that at this pressure range, the generator is working at around 10% of its nominal condition, a region where the losses are high. For RMS-Δ_p over 6.2 kPa, CL6 shows an exponential trend that follows the turbine power curve. No valid tests over 6.2 kPa were found for CL1.

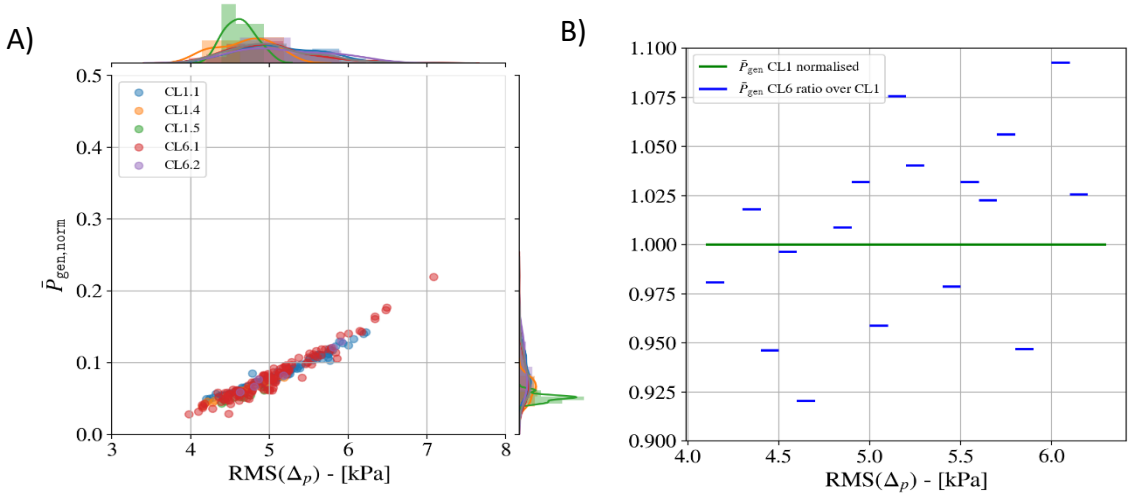

FIGURE 30. CL1-CL6 COMPARISON OF AVERAGE GENERATOR POWER: A) IN FUNCTION OF THE PRESSURE VARIATION AND B) WITH BIN COMPARISON

During the Mutriku tests, the predictive CL6 law showed production improvement in comparison with CL1 of around 30%. The performance results in BiMEP are not so convincing in the direct comparison with CL1. Possible ways of improvements can be:

- The wave forecasting was not accurate enough to compute the excitation forces. In the current version of the algorithm, the wave propagation time was computed assuming cylindrical waves travelling with the most frequent wave direction. Plus, the force estimation was done with the numerical model;
- The model was not perfectly adjusted to replicate the exact behaviour of the real system and relied on the linear wave theory assumptions;
- CL1 was better tuned and the various versions rightly employed in function of the conditions in presence.

During the BiMEP tests, CL6.1 and CL6.2 presented similar production performance. The most important conclusion resided in the fact CL6.2 performed as expected with a significant improvement in terms of implementation because all the optimisation code was embedded into the PLC. This leads to a reduction of the risk related to a failure in the external PC or the communication between them.

4.2.3 CL OVERALL COMPARISON

4.2.3.1 CL BEHAVIOUR

This section details the behaviour of each control law by associating the pneumatic power and the turbine speed as presented in Figure 31. Pneumatic power versus average turbine speed. The higher generator torques applied by CL2 resulted in lower rotational speeds for similar values of P_{pneu}. The lower rotational speeds resulted in lower turbine efficiencies, but it also led to higher generator efficiencies. It would also help to suppress rotational speeds in higher energy conditions, which could maintain operating conditions of the PTO by avoiding turbine overspeed. Regarding CL6, three trends of applied damping are visible. This is the result of the automatic optimisation of the control parameters which adapts them in function of the sea states. Only the main trend was selected by the processing algorithm, representing the highest accuracy between the computed and applied torque. The two other trends below 40% of the average turbine speed were simply discarded by the post-processing.

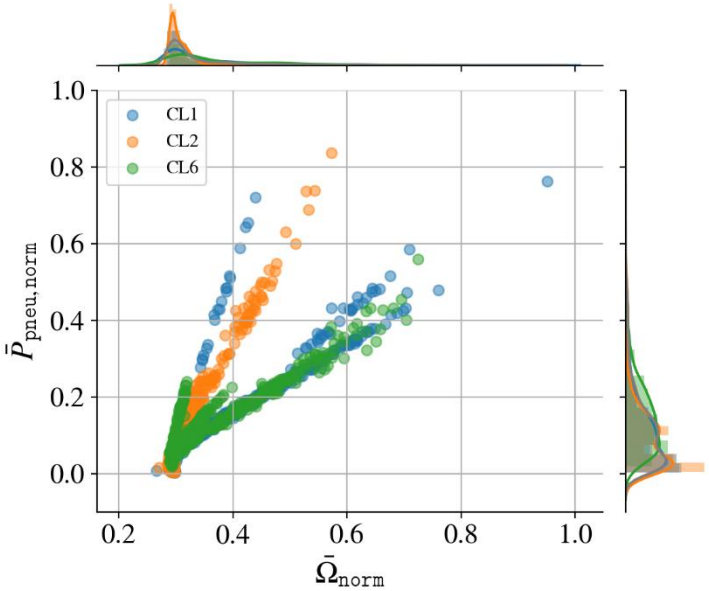

FIGURE 31. PNEUMATIC POWER VERSUS AVERAGE TURBINE SPEED FOR THE ENTIRE SET OF TESTS

4.2.3.2 POWER PRODUCTION

Power production here is heavily influenced by dataset selection. Under similar control conditions, an electrical power curve is presented in Figure 32 as a function of the RMS value of the pressure variations. It can be shown the curve follows a cubic trend and a potential regression gives the relation

$$P_{gen} \approx 6.10^{-4} {p_{ch}}^3$$

CL2 was the controller with the selected data producing the higher average electrical output.

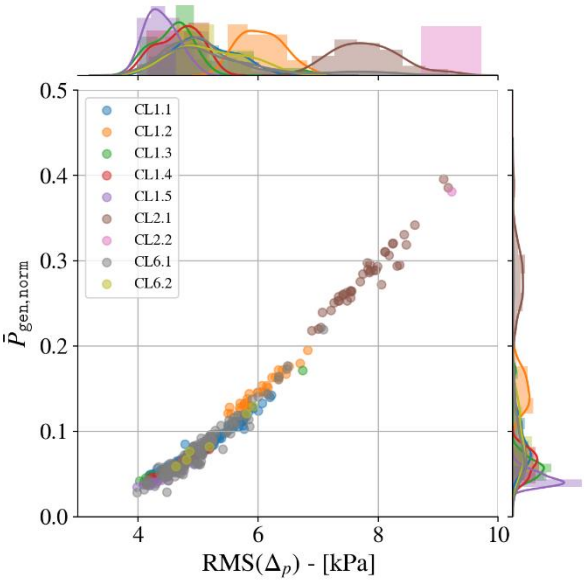

FIGURE 32. AVERAGE ELECTRICAL POWER OUTPUT GENERATED FOR EACH CL

4.2.3.3 PTO EFFICIENCIES

The plot for the turbine and generator efficiencies for the various control law tests evaluated during MARMOK-A-5 testing show similar results to the Mutriku Phase II testing. The data in Figure 33-A) indicate that CL2 turbine efficiencies ranged from approximately 50 to 53%, much lower than CL1 and CL6, which ranged from approximately 54 to 60%. Meanwhile in Figure 33-B), the generator efficiency for CL2 ranged from 50 to 60%, which is much higher than CL1 and CL6 which ranged from approximately 10 to 50%.

Overall the PTO efficiencies of CL2 ranged from approximately 25 to 32%, while for CL1 and CL6 PTO efficiencies range from approximately 5 to 30%. These results are consistent with the results of the Mutriku Phase II tests and indicate that, under open loop control, the losses in turbine efficiency caused by CL2 are outweighed by the gains in generator efficiency. In Mutriku Phase I, the maximum PTO efficiency of CL1 was 49%, while CL2 and CL5 obtained 47% and 45%, respectively. This indicates the negative effect of the d*V*/d*t* filter in the generator power. Figure 17 demonstrates that the generator efficiency has decreased between Mutriku Phase I and the subsequent tests during Mutriku Phase II and at BiMEP.

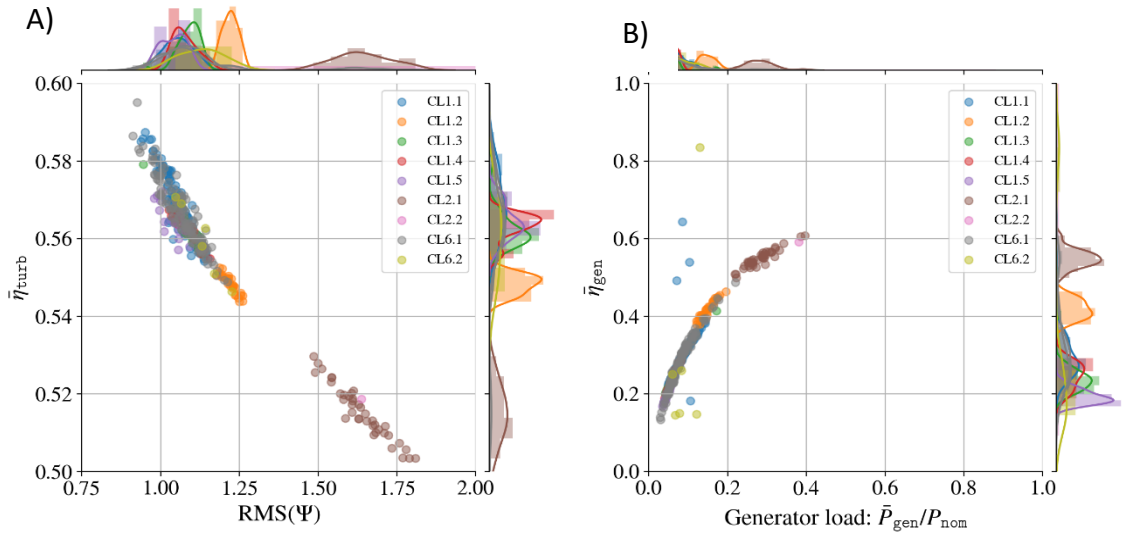

FIGURE 33. GLOBAL PTO EFFICIENCIES FOR EACH CL WITH A) THE TURBINE AND B) THE GENERATOR

4.2.3.4 RELIABILITY ISSUES

The reliability issues evaluated were focused on the following main criteria:

- Occurrence of overspeed events: although the safety valve control avoided the drive train to reach high speeds, the generator had a maximum rotational speed during operation that it could not overshoot; also, it was sensitive to vibration produced at elevated speeds, beyond which there was a risk of contact between the rotor and the stator;
- Application of high generator torque and generator power loads: these quantities allow the assessment of the cases close to nominal conditions and if they were overpassed;
- Standard deviation of generator power output: it represented the probability dispersion of results, meaning how far from the average power production the power peaks appeared.

In all aspects CL2 performed better than CL1 and CL6.

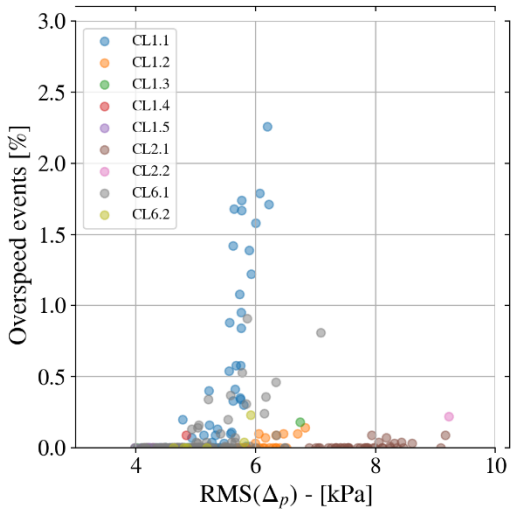

Figure 34 shows the number of overspeed events for each dataset evaluated for this deliverable. It indicates the capability of the CLs to brake the turbine, preventing it from overreaching the threshold and as a consequence reducing the dependence of the system on the safety shut-off valve. Globally the results present very few events of overspeed. CL1.1 had a higher probability in reaching that operational limit with some cases where 2.3% of collected values within a test reached the speed limit. CL6 had few cases below 1% of overspeed events.

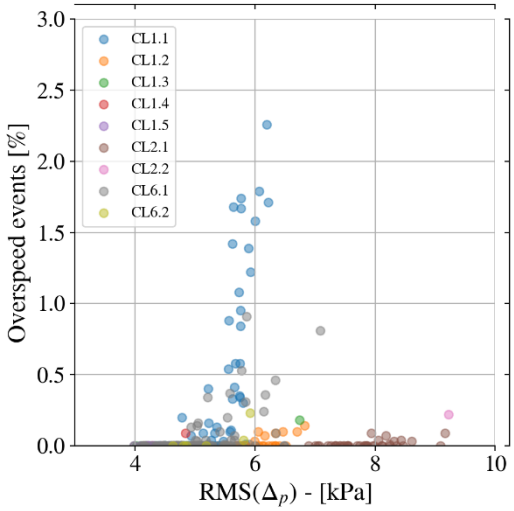

FIGURE 34. EVALUATION OF THE OVERSPEED EVENTS

Despite being operated under higher pressure and higher energy conditions, CL2 resulted in fewer overspeed events than CL1 and CL6, which is better for the longevity of the PTO system, as well average power generation because it avoids using the safety shut-off valve.

Figure 35-A) and Figure 35-B) present respectively the averages of the highest 5% of normalised torque and power applied to the electrical generator, while Figure 36 is the standard deviation of the electrical power output of the generator. While in nearly all cases,

CL2 results in higher values of torque, power, and power standard deviation, these values occurred at higher generator loads, which means higher power inputs to the PTO. If the data were extrapolated out to observe overlapping conditions, the results for CL2 would be lower in all cases when compared to CL1 and CL6, particularly for electrical power output. This indicates that CL2 does not stress the generator and power electronics has much as the competing controls. The reliability analysis indicates CL2 should result in less wear on both electrical and mechanical equipment, which would result in longer life and greater availability of the PTO compared to the application of CL1 and CL6.

CL6 was configured to find the best control parameters minimizing the objective function without restrictions. In simulation works, constraints were introduced to discard the torque law parameters that would produce generator power above a selected threshold. This feature was not tested in BiMEP but would be a recommendation for lowering the probability of operation in higher torques and powers. The results in Figure 35-B) shows most of the CL1 and CL6 cases an average of the 5% of maximum power levels below 75%. Only one case of CL6 where power levels reached the nominal power. This occurred for generator loads lower than for CL2.

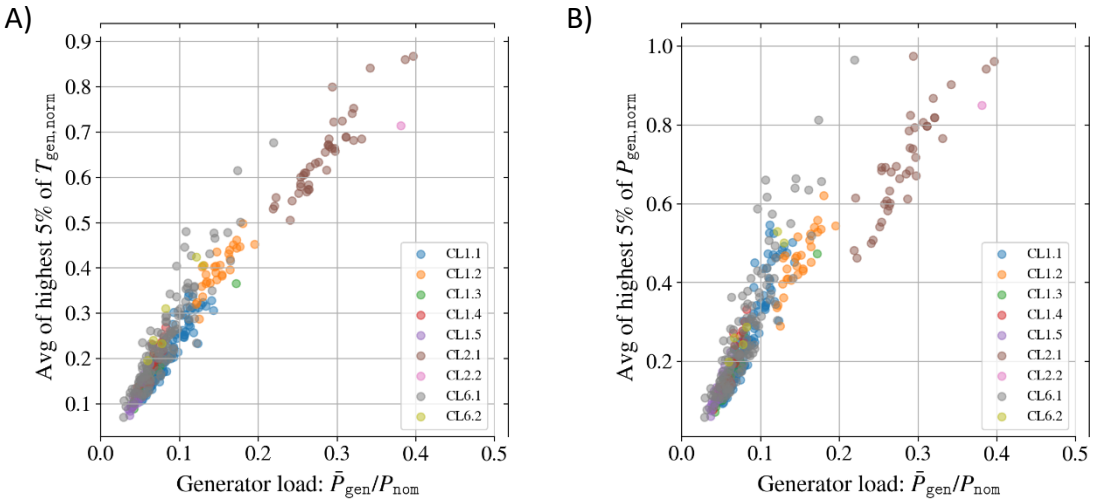

FIGURE 35. AVERAGE OF THE HIGHEST 5% OF NORMALIZED GENERATOR A) TORQUE AND B) POWER AS A FUNCTION OF THE GENERATOR LOAD FOR EACH CL

The standard deviations of the normalised electrical power are presented in Figure 36 for all the controllers. A high number indicates an operation with higher power peaks with respect to the average power output. The trends of each CL are therefore quite similar to the Figure 35 B), and so are the observations.

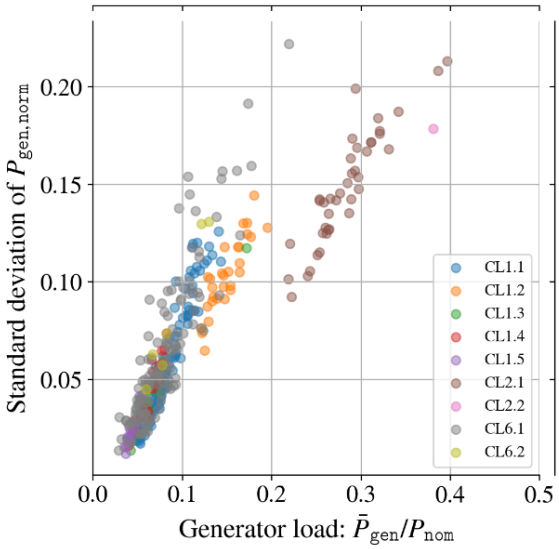

FIGURE 36. STANDARD DEVIATION OF ELECTRICAL POWER FOR EACH CL

4.2.4 GLOBAL EVALUATION

The analysis focused on two main aspects influenced by the control strategies: the PTO performance and the reliability of its components in high operation regions.

Regarding the CL performance, during Phase I several versions of CL1 and CL2 were tested. The tests considered valid highlighted CL1 operated in ranges of pressures lower than CL2, higher turbine speeds and consequently lower dimensionless pressure head Ψ. Direct comparison was therefore not directly feasible unless using dimensionless parameters on the PTO efficiencies. The conclusions are:

- CL1 managed to operate the turbine at highest average efficiency within a range between 54% to 58% where CL1.3 and CL1.5 were the most efficient versions;
- Within the versions of CL1, and although it presented turbine efficiencies close to 55%, CL1.2 operated higher output electrical power because it operated the generator at higher load regimes and consequently higher generator efficiencies;
- Although CL2 did not present average turbine efficiencies higher than 53%, it obtained the highest ranking when focusing on the generator average efficiency between 50% to 60%, mainly because the valid tests operated at higher pressure values at the PTO input, applied higher torque/speed ratios and thus higher generator loads.

During Phase II of tests, CL1 versions CL1.1, CL1.4 and CL1.5 were operated along with CL6. Globally they presented a similar behaviour and only slight differences were detected in the selected tests:

- CL1 globally showed slightly better performance in turbine efficiency thanks to a more efficient CL1.1;

- CL6 presented the highest average efficiency during an individual test almost reaching 60%;
- CL6 operated at slightly higher generator efficiencies and the electrical output was globally a bit better with few tests at higher generator loads.

During both phases, the conditions did not allow the operation of the generator at an average load higher than 40%.

Regarding reliability issues, no failure nor damage was witnessed in the drive train during the BiMEP test where the highest safety measures were assured. The study focused on turbine overspeed events and operation at high generator torques and powers. Note that the common valve control prevented from reaching the maximum generator rotor speed. Analysing the reliability results, we can state that:

- While CL1 was more likely to let the turbine rotates at higher speeds, therefore applying lower torques, it presented the lowest figures in terms of power levels and standard deviation of output power;
- Nearly no overspeed events were detected in the valid tests of CL2 and CL6;
- As a consequence, they presented a higher probability of having torque and power levels close to the rated values;
- CL6 reached the generator limits at early load regimes.

5. LESSONS LEARNT AND RECOMMENDATIONS

This section collects the key points on the lessons learnt during the different testing phases of the PTO in BiMEP and aim at proposing a return on experience focused on the experimental work of the control algorithms. The following points support the success of the open sea trials of the controllers in the MARMOK-A-5:

- Operational data were easily accessible in the production databases. It is of paramount importance to rely on the highest quality of data continuously available, and the database proved to be the best candidate to collect the process variable along the overall period of tests (Mutriku and BiMEP);
- It allowed a reactive tuning of the control algorithms on-the-go, and several versions of CL1 and CL2 could be tested which enhanced the testing opportunities;
- A first of its kind predictive controller for OWC systems was operational at sea with measurement buoy data sent real time. The CL6.2 version of the non-linear predictive control was directly implemented in the PLC without additional PC to perform the online computation;
- The controllers could be tested in a variety of sea states although concentrated in late spring. The MARMOK-A-5 buoy was available 90% of the time after the full commissioning and allowed 2239 individual CL tests.

The trials took place in an offshore environment where the environmental conditions limit the accessibility of the installation and the highest safety measures were essential. Special attention on certain aspects as listed below were required along with their consequence on the testing period:

- The commissioning took longer than expected, the HSSV early operation not complying the levels of safety for offshore testing. Issues in the valve control software and the hardware (actuator motor, junction box) were solved. After that the sea trials had non-stop autonomous operation without suffering any failure;
- As a preventive action the valve actuation time was increased and did not allow the test of the latching controllers.

The main limitations experienced during the Mutriku Phase II tests and in BiMEP came from the generator failure in Mutriku after 3 months of operation during Phase I test. A high voltage peak provoked a shortcut in the stator windings and after the repair including the proper insulation of the stator winding, the manufacturer advised the installation of a dV/dt filter between the generator and the power electronics. Here are listed the consequences of that change with respect to the prior installation:

- The installation of the electrical filter le to a change of the power electronics inner current control to an open-loop approach with lower accuracy in low generator operation regions;
- A post-processing algorithm for sorting valid tests had to be developed. The individual tests were considered 'valid' when the reference torque calculated by the controllers was equivalent to the one actually applied at the generator. The algorithm discarded operation in motor mode when the turbine was rotating at low rotational speed following the recommendations of deliverable D3.4;
- The criteria imposed by the processing allowed 16% of tests to be assessed.

6. CONCLUSIONS

The present deliverable focuses on the open sea trials of the control algorithms tested to operate the PTO, composed of the biradial turbine, installed on the MARMOK-A-5 buoy at the BiMEP test site. Thanks to the knowledge acquired from the Mutriku test campaign, the controllers were fine-tuned for this new framework, and several versions could be tested.

The control algorithms tested were the adaptive controllers CL1 (selected to as the baseline) and CL2; and the predictive algorithm CL6, which is a first its kind predictive algorithm to be deployed in a WEC using wave measurement up-wave to provide an online optimisation. With the objective of allowing comparison between the controllers, the testing period was divided into two phases where CL1-CL2 and then CL1-CL6 were tested. After some delays in the completion of the Power Take-Off commissioning at sea were experienced, mainly due to the higher safety approach imposed by the offshore environment and the waiting time for suitable weather windows, a total rounding the 900 hours of operation representing a 90% availability of the buoy were amassed during Spring 2019. Although there was a variety of sea states, the wave resource was rather calm with an average significant wave height of 1.30 m associated with an average energy period of 7.16 s. In these conditions, the PTO system operated at partial load for all the controllers.

The results were presented in the form of a performance and a reliability assessments. While the performance evaluation focused on the components' efficiencies and the electrical power output, the reliability one focused on extreme events and stresses to the PTO as no failure was experienced. The comparison between the CLs was only made in function of process variables or measured quantities because the wave resource was not available due to Intellectual Property reasons. A post-process algorithm had to be devised to select only the tests considered as valid upon the criteria of the correct application of the generator torque calculated by the controllers. Indeed, after the generator failure during the Mutriku Phase I test, an electrical filter was installed which forced the inner current controller of the power electronics to be modified from a closed-loop system to an open-loop system. This type of control was found to be less accurate at low operation regions and led to the generator operating below its usual efficiency range as highlighted in Deliverable D3.4. In the end, 15% of the total tests were selected by the process algorithm.

Focusing on the turbine performance, a maximum average efficiency for an individual test of nearly 60% was obtained during the operation of CL6. The several versions of CL1 and the CL6 presented similar results in terms of operation ranges and efficiency results, the average turbine efficiency ranging from 54% to almost 60%. In the meantime, CL2 presented figures between 50% and 53%. Due to CL2's intrinsic operation behaviour, the CL2 test results are situated at higher pressure ranges with no common operation point with the baseline controller. In terms of generator efficiency, CL2 presented valid tests at higher load regimes

with the highest figures in comparison with the other control laws. Average generator efficiency results are between 50% and 60% at generator loads between 20% to 30% while CL1 and CL6 presented results only until a 20% load. Although direct comparison with CL1 would lead to speculation, the trend suggests that CL2 resulted in better performance in terms of electrical output although there were not enough valid tests to prove this. After Mutriku testing, the predictive controller CL6 produced 30% of electrical power output more than the base case. This figure was not reproduced in BiMEP and we are investigating why this is the case and we want to improve the accuracy of the wave force predictor (both in the estimator and the propagation of incident waves) and dispose of a fully validated Wave-to-Wire numerical model.

7. REFERENCES

[1] F.-X. Faÿ *et al.*, 'OPERA D4.2 - Shoreline OWC wave power plant control algorithms', Jul. 2018.
[2] L. M. C. Gato, A. A. D. Carrelhas, J. C. C. Henriques, B. S. Lopes, J. Varandas, and F.-X. Faÿ, 'OPERA D3.3 - Turbine and electrical equipment performance and reliability in shoreline OWC wave plant', Jul. 2018.
[3] J. C. C. Henriques, L. M. C. Gato, A. A. D. Carelhas, and J. Varandas, 'OPERA D3.4 - Open-sea performance and reliability of the OWC turbine and electrical equipment', Jul. 2019.
[4] L. M. C. Gato, A. A. D. Carrelhas, F. X. C. da Fonseca, and J. C. C. Henriques, 'OPERA D3.2 - Turbine-generator set laboratory tests in variable unidirectional flow', Jun. 2017.
[5] 'Recommended Practice DNV-RP-C205: Environmental Conditions and Environmental Loads', 2007.
[6] J. Falnes, *Ocean waves and oscillating systems*. Cambridge University Press, 2002.
[7] B. Guo, R. J. Patton, S. Jin, and J. Lan, 'Numerical and experimental studies of excitation force approximation for wave energy conversion', *Renew. Energy*, Mar. 2018.
[8] J. Berque, P. Ruiz-Minguela, D. Crooks, and F. Thiebaut, 'OPERA D5.3 - Uncertainty in Wave Energy Converter Power Performance Assessment', May 2019.